Natural Resources Canada | Ressources naturelles Canada

GEOLOGICAL SURVEY OF CANADA
OPEN FILE 8403

Geology of the Cheechoo gold property, Eeyou Istchee Baie-James, Superior Province, northern Quebec

A. Fontaine, B. Dubé, M. Malo, J. Turcotte, and D. Doucet

2018

Canada

GEOLOGICAL SURVEY OF CANADA
OPEN FILE 8403

Geology of the Cheechoo gold property, Eeyou Istchee Baie-James, Superior Province, northern Quebec

A. Fontaine[1], B. Dubé[2], M. Malo[1], J. Turcotte[3], and D. Doucet[3]

[1] Institut national de la recherche scientifique, 490 rue de la Couronne, Québec, Quebec G1K 9A9
[2] Geological Survey of Canada, 490 rue de la Couronne, Québec, Quebec G1K 9A9
[3] Sirios Resources, 1000 rue Saint-Antoine Ouest (suite 410), Montréal, Quebec H3C 3R7

2018

Permanent link: https://doi.org/10.4095/308244

This publication is available for free download through GEOSCAN (http://geoscan.nrcan.gc.ca/).

Recommended citation
Fontaine, A., Dubé, B., Malo, M., Turcotte, J., and Doucet, D., 2018. Geology of the Cheechoo gold property, Eeyou Istchee Baie-James, Superior Province, northern Quebec; Geological Survey of Canada, Open File 8403, 25 p. https://doi.org/10.4095/308244

Publications in this series have not been edited; they are released as submitted by the author.

Geology of the Cheechoo gold property, Eeyou Istchee Baie-James, Superior Province, northern Quebec

Arnaud Fontaine[1]*, Benoît Dubé[2], Michel Malo[1], Jordi Turcotte[3] and, Dominique Doucet[3]

[1] *Institut national de la recherche scientifique, 490 rue de la Couronne, Québec, Quebec G1K 9A9*
[2] *Geological Survey of Canada, 490 rue de la Couronne, Québec, Quebec G1K 9A9*
[3] *Sirios Resources, 1000 rue Saint-Antoine Ouest (suite 410), Montréal, Quebec H3C 3R7*
**Corresponding author's e-mail: arnaud.fontaine@ete.inrs.ca*

Contribution to the Geological Survey of Canada's Targeted Geoscience Initiative 5 (TGI-5) Program (2016–2020)

ABSTRACT

The Cheechoo property (Sirios Resources) is located at 15 km southeast of the Éléonore world-class gold mine (reserves and resources of 7.1 Moz Au). The property is mainly underlain by paragneissic wacke and migmatites belonging to the Opinaca Subprovince, local banded iron formations and mafic dykes of the La Grande Subprovince, and the Cheechoo intrusion. The Cheechoo intrusion is dated at 2612 Ma, which is penecontemporaneous with the 2618 Ma Vieux Comptoir suite and the 2620-2600 Ma leucogranitic dykes and veins that are injected within the supracrustal rocks of the La Grande Subprovince during amphibolite facies metamorphism. Locally, the Cheechoo intrusion shows a progressive transition and consanguineous relationships with quartz-feldspar pegmatite dykes. The later dykes are concentrated at the margins of the Cheechoo intrusion and spatially associated with part of the gold mineralization. These dykes have a high variation of mineral assemblages and miarolitic cavities suggesting crystallization near or at the magmatic-hydrothermal transition. The Cheechoo intrusion has variable textures from massive, porphyritic with feldspar phenocrysts to gneissic and sacharoidal with biotite porphyroblasts, suggesting a complex magmatic and metamorphic history. Lithogeochemical data indicates that the intrusion has granodioritic, trondjemitic, metaluminous to peraluminous compositions, reduced nature ($Fe_2O_3/FeO < 0.2$) and REE patterns, similar to some leucogranites of the Opinaca Subprovince. The high Na_2O content (> 6 wt %) of the Cheechoo intrusion can be attributed to an early-Au sodic metasomatic event. Detailed mapping of stripped outcrops indicate that gold-bearing zones are mainly hosted by the Cheechoo intrusion and to a lesser extent within surrounding metasedimentary rocks, pegmatite dykes and mafic schists. Gold mineralization is characterized by a network of sheeted quartz±(feldspar) veins with variable amounts of phlogopite, actinolite, diopside and scheelite that are related to calc-silicate and potassic alteration halos, mainly developed in vein selvages. High-grade gold veins and their selvages generally contain less than 5 % of disseminated sulphides (arsenopyrite, pyrrhotite ± pyrite) and have a coarse pegmatitic texture with local visible gold (similar to the Moni prospect). Cross-cutting relationships between gold-bearing sets of veins indicates an early V_1 veins network composed of quartz ± (feldspar, actinolite, scheelite, pyrite, pyrrhotite, arsenopyrite), followed by sheeted, extensional to en-echelon V_2 veins network (60-70% of the veins) characterized by quartz ± (feldspar, phlogopite, pyrrhotite and arsenopyrite). The V_2 veins are cut by V_3 extensional veins, composed of quartz ± actinolite. Gold mineralization has a Bi-W-As ± (Te, Se, Pb) metallic signature in association with Mg-K enrichments associated with narrow alteration zones in vein selvages. In-situ $\delta^{34}S$ analyses of gold-associated sulphides are similar to those of typical Archean orogenic gold deposits and to values of sulphides from the Éléonore gold mine, thus suggesting fluid(s) of similar compositions. The age of the host Cheechoo intrusion, 2612 Ma, represents the maximum age of gold mineralization. The structural characteristics of the auriferous system are best explained by a model of syn-tectonic (late-D_2) emplacement of the Cheechoo intrusion and related leucogranitic dykes and gold-bearing veins networks. The mineralogy of the auriferous veins, the hydrothermal alteration assemblages and the spatial association with the reduced intrusion, pegmatite dykes and mafic schists bare similarities with those of reduced intrusion-related gold systems. The Cheechoo property represents a new style of gold mineralization in the Eeyou Istchee Baie-James municipality.

RÉSUMÉ

La propriété Cheechoo (Ressources Sirios) est située à 15 km au sud-est de la mine d'or de classe mondiale Éléonore (réserves et ressources de 7,1 millions d'onces d'or). La propriété est principalement constituée de wacke paragneissique, de migmatites (sous-province de l'Opinaca), de formations de fer rubannées, de dykes mafiques et de l'intrusion de Cheechoo (Sous-province de La Grande). L'intrusion de Cheechoo est datée à 2612 Ma, pénécontemporaine de la suite du Vieux-Comptoir (2618 Ma) et des dykes et veines leucogranitiques (2620-2600 Ma), injectés dans les roches supracrustales de la Sous-province de La Grande lors du métamorphisme aux faciès des amphibolites. Localement, l'intrusion de Cheechoo montre une transition progressive et des relations consanguines avec des dykes de pegmatites à quartz et feldspath. Ces derniers sont concentrés aux bordures de l'intrusion de Cheechoo et spatialement associés à une partie de la minéralisation aurifère. Ces dykes présentent une forte variabilité minéralogique et localement, des cavités miarolitiques, suggérant une cristallisation à proximité ou à la transition magmatique-hydrothermale. L'intrusion de Cheechoo présente des textures variables allant d'une texture massive, à porphyrique à feldspaths, à gneissique et saccharoïde avec des porphyroblastes de biotite. Ces textures suggèrent une histoire magmatique et métamorphique complexe. Les données lithogéochimiques indiquent que l'intrusion a une composition granodioritique, trondhjémitique, métalumineuse à péralumineuse, réduite (Fe_2O_3 / FeO <0,2) et des patrons de terres rares, similaires à certains leucogranites de la Sous-province Opinaca. La teneur élevée en Na_2O (> 6 % poids d'oxydes) de l'intrusion de Cheechoo peut être attribuée à un événement métasomatique sodique précoce. La cartographie détaillée des tranchées indique que les zones aurifères sont principalement encaissées dans l'intrusion de Cheechoo et, dans une moindre mesure, dans les roches métasédimentaires environnantes, et au sein des dykes de pegmatites et des schistes mafiques. La minéralisation aurifère est caractérisée par un réseau de veines et veinules de quartz ± feldspath (« sheeted vein array ») avec des quantités variables de phlogopite, d'actinolite, de diopside et de scheelite, formant des halos d'altération calco-silicatés et potassiques. Les veines aurifères à haute teneur et leurs épontes contiennent généralement moins de 5 % de sulfures disséminés (arsénopyrite, pyrrhotite ± pyrite) et une texture pegmatitique avec parfois, de l'or visible (similaire à l'indice Moni). Les relations de recoupement entre les veines aurifères indiquent un réseau précoce de veines V_1 composé de quartz ± (feldspath, actinolite, scheelite, pyrite, pyrrhotite, arsénopyrite), suivi d'un réseau de veines V_2 en extension et en-échelon (60- 70% des veines), caractérisé par du quartz ± (feldspath, phlogopite, pyrrhotite et arsénopyrite). Les veines V_2 sont recoupées par des veines extensionnelles V_3, composées de quartz ± actinolite. La minéralisation aurifère a une signature métallique Bi-W-As ± (Te, Se, Pb) en association avec des enrichissements en Mg-K, associés à des zones d'altération restreintes aux épontes des veines. Les analyses $\delta^{34}S$ in situ des sulfures associés à l'or ont des valeurs similaires à celles des gisements aurifères orogéniques typiques de l'Archéen et aux sulfures de la mine d'or Éléonore, suggérant des fluides de compositions similaires. L'âge de l'intrusion de Cheechoo, 2612 Ma, représente l'âge maximum de la minéralisation aurifère. Les caractéristiques structurales du système aurifère peuvent s'expliquer par un modèle de mise en place syn-tectonique (tardive-D_2) de l'intrusion Cheechoo et des réseaux de dykes leucogranitiques et des veines aurifères. La minéralogie des veines aurifères, les assemblages d'altération hydrothermale et l'association spatiale avec l'intrusion réduite, les dykes de pegmatite et les schistes mafiques sont des caractéristiques partagées avec les systèmes aurifères associés à des intrusions réduites. La minéralisation aurifère au sein de l'intrusion réduite de Cheechoo, datée à 2612 Ma, représente un nouveau style de minéralisation aurifère dans la municipalité de Eeyou Istchee Baie-James.

INTRODUCTION

The Cheechoo property (Sirios Resources) is located in the Eeyou Istchee Baie-James municipality, 15 km southeast of the Éléonore mine (Fig. 1). Sirios Resources acquired the Cheechoo property in 2004, just after the announcement of the Roberto showing discovery by Mines d'Or Virginia. From 2005 to 2011, Golden Valley Mines, the property operator, conducted an exploration program including electromagnetic and aeromagnetic surveys, ground magnetometric survey, conventional prospecting, trenching, channel sampling, humus geochemistry, and drilling (Turcotte, 2014). Between 2010 and 2012, systematic prospecting by Sirios Resources, Golden Valley Mines and IOS Services Géoscientifiques Inc. led to uncovering numerous gold-bearing samples (Turcotte, 2014). In 2013, a drilling campaign intersected an interval of 41 meters at 0.74 g/t Au (Turcotte, 2014). Between 2014 and 2018, more drill hole intersections confirm the presence of an auriferous system, including 1.53 g/t Au over 19.5 m (Sirios, 2014), 12.8 g/t Au over 20.3 m (Sirios, 2016), 11.9 g/t Au over 13.5 m (Sirios, 2017), 41,0 g/t Au over 8 m (Sirios, 2018c) and 56.4 g/t Au over 8.2 m (Sirios, 2018a). In 2016, Sirios Resources team was awarded the "discovery of the year" by the Quebec Mineral Exploration Association (AEMQ) for the Cheechoo gold project. In 2017, other showings were discovered along the intrusion margins (6-9, 2-2, and November showings) and within the intrusion (mafic dyke showing). About 2000 metres of channel sampling was completed on the main stripped area (Fig. 2), which gave a weighted average Au grade of 0.4 g/t (Sirios, 2018b). The Cheechoo and Éléonore South (Azimut/Goldcorp/Eastmain joint venture) properties are interpreted to share the same auriferous system centered on the Cheechoo intrusion (Fontaine et al., 2017b).

Gold deposits in metamorphosed and deformed terranes are associated with a wide range of host rocks that are typically associated with major structures in greenschist facies zones (Colvine, 1989; Groves et al., 1990; Poulsen et al., 2000; Goldfarb et al., 2005; Robert et al., 2005; Dubé and Gosselin, 2007; Dubé et al., 2015). However, some are hosted by amphibolite or granulite facies metamorphic rocks (Couture and Guha, 1990; Barnicoat et al., 1991; Groves, 1993; Neumayr et al., 1993; Poulsen et al., 2000; Goldfarb et al., 2005; Dubé and Gosselin, 2007), like world-class Canadian gold deposits such as Hemlo, Lupin, Musselwhite, and Éléonore, where genesis remain relatively controversial (Dubé et al., 2015). Critically reassessing this so-called "atypical" type of gold mineralization in high-grade metamorphic terrains may lead to new exploration models (Dubé et al., 2015).

The study of the Cheechoo property is an opportunity to unravel a new style of gold mineralization in the Éléonore area and the potential influence of magmatism on gold mineralization (Fontaine et al., 2017a). A better understanding of the nature, distribution and origin of gold mineralization is critical for exploration. In-depth descriptions of the Cheechoo gold mineralization could help to test some hypotheses such as 1) is the gold system orogenic and/or syn-magmatic, 2) is the bulk of the gold mineralization pre- to syn-peak of metamorphism and, 3) is mineralization the product of distinct or polyphase event(s). This report focuses on detailed mapping conducted on the main stripping area and the 6-9 trench of the Cheechoo property. The regional setting of the deposit is briefly presented in order to provide a framework for trench descriptions. Geological maps of stripped outcrops are presented and discussed with an emphasis on structural features and timing relationships with the auriferous vein network. Lithogeochemical features of the intrusion are also discussed and compared to similar intrusions in the area. The vein network, hydrothermal alteration and their geochemical footprints are also described, using macroscopic and petrographic observations, mass balance calculations and the sulfur isotope composition of gold-associated sulphides. Finally, structural controls of the auriferous vein network, geochemical features of the intrusion and analogies with similar gold mineralization are discussed.

REGIONAL GEOLOGY

The Eeyou Istchee Baie-James municipality is a vast area of about 335 000 km^2 mainly comprising the La Grande and the Opinaca Subprovinces, and the northern part of the Opatica and the Nemiscau Subprovinces. The study area is located at the boundary between the La Grande and Opinaca Subprovinces (Fig. 1), which is defined by: i) a gradual transition from greenschist to upper amphibolite and granulite metamorphic rocks (Gauthier et al., 2007; Bandyayera et al., 2010), ii) a regional aeromagnetic discontinuity (Bandyayera et al., 2010), and iii) the appearance of orthopyroxene and migmatites in the paragneissic rocks to the north (Bandyayera et al., 2010). Locally, the contact is obscured by tonalite and granodiorite intrusions (Hocq, 1994), such as the Janin and Boyd suites or the Rotis and Menouow intrusions (Bandyayera and Fliszár, 2007; Bandyayera and Lacoste, 2009; Bandyayera et al., 2010).

The La Grande Subprovince

The La Grande Subprovince is separated into a northern (La Grande River) and a southern domain (Eastmain River) (Gauthier and Larocque, 1998). These domains consist of Paleo- to Mesoarchean basement, overlain by Meso- to Neoarchean volcano-sedimentary sequences and injected by syn- to late-tectonic intrusions (Card and Ciesielski, 1986; Hocq, 1994; Goutier et al., 2001). The La Grande River domain is interpreted to reflect a peri-cratonic environment, located directly to the south of the "Superior proto-craton" (Card, 1990; Percival et al., 1994; Stern et al., 1994; Gauthier, 2000). The Eastmain River domain has been mapped and studied in detailed by the Geological Survey of Canada (Low, 1896) and the Ministère de l'Énergie et des Ressources Naturelles (Remick, 1977; Franconi, 1978; Simard and Gosselin, 1999; Moukhsil, 2000; Moukhsil et al., 2003). The Eastmain River domain is characterized by greenstone belts composed of four volcanic cycles dated from 2752 to 2703 Ma comprising komatiitic to rhyolitic lavas and tuffs with tholeiitic to local calk-alkaline affinities (Moukhsil et al., 2003). Conglomerate and turbiditic wacke (Roberto host rocks) containing local iron-rich units of the Low Formation overlie volcanic sequences (Franconi, 1978; Moukhsil et al., 2003; Bandyayera and Fliszár, 2007). Gold exploration activity is focused on the La Grande Subprovince and its margins with the Opinaca and Nemiscau Subprovinces, and within the Middle and Lower Eastmain belt, the largest greenstone belt in the Eeyou Istchee Baie-James municipality.

The Opinaca Subprovince

The Opinaca Subprovince occurs between the Eastmain domain to the south and the La Grande domain to the north. The Opinaca belongs to metasedimentary belts, interpreted as accretionary prisms, such as the Quetico, the Nemiscau and the Ashuanipi Subprovinces (Card, 1990; Williams, 1990; Goutier et al., 2001; Thurston, 2002; Percival et al., 2012; Morfin et al., 2014). The Opinaca Subprovince covers 35 000 km^2, characterized by paragneiss and migmatites, intruded by syn- to post-tectonic, locally ultramafic intrusions (Simard and Gosselin, 1999; Bandyayera and Fliszár, 2007; Morfin et al., 2013). Tonalitic to granitic intrusions and leucogranitic dykes and veins have a S-type peraluminous composition, suggesting a derivation from partial melting of metasedimentary rocks and fractionated magmas (Moukhsil et al., 2003; Morfin et al., 2014). The Opinaca Subprovince has been interpreted as an injection complex by Morfin et al. (2013, 2014). As defined by Weinberg and Searle (1998), an injection complex is an accumulation of evolved anatectic melt in the lower crust, at a depth close to the solidus (Morfin et al., 2014). The timing of episodic partial melting is constrained between 2671 Ma, the age of the oldest metamorphic zircons and the 2637 Ma intrusion of leucogranitic dykes and veins, coeval with the main D_2 phase of deformation in the Opinaca (David et al., 2010; Morfin et al., 2013). This long-lived tectonometamorphic event was first initiated in the highly metamorphosed core of the Opinaca Subprovince (Morfin et al., 2013) and later along its margins, within the lower grade La Grande Subprovince supracrustal rocks at 2620-2600 Ma (Dubé et al., 2011). Evidence of retrogression (hydration of orthopyroxene into biotite and/or amphibole) is restricted to late shear zones (Simard and Gosselin, 1999; Morfin et al., 2013). These shear zones are locally truncated by younger granitic and granodioritic intrusions (Morfin et al., 2013), associated with the Vieux Comptoir granitic with younger phases (nAvcr2) dated between 2640 and 2613 Ma (David and Parent, 1997; Goutier et al., 1999; Goutier, 2017).

Leucogranitic dykes and veins of the Opinaca Subprovince have been interpreted as highly evolved leucogranites formed by partial melting of metasedimentary source, experienced an early fractional crystallization of plagioclase (Morfin et al., 2013; Morfin et al., 2014). Those intrusions are distinguished from the Tonalite-Trondjhemite-Granodiorite (TTG) suite that originated from melting of subducted oceanic crust (Condie, 1981; Jahn et al., 1981), such as the Desliens igneous suite in the Ashuanipi Subprovince (Percival et al., 2003), based on their Ni content, generally < 15 ppm (Morfin et al., 2014) and MgO content (< 2 wt %). The Vieux Comptoir suite (nAvcr2) is composed of ovoids alkaline granite and granite, containing biotite and magnetite, with youngest phases dated between 2640-2613 Ma (Goutier et al., 1999; Goutier, 2017). Those intrusions can contain up to 10% of tonalitic enclaves (Goutier et al., 1999; Bandyayera and Lacoste, 2009). The Rotis pluton, dated at 2671 Ma (David et al., 2010), is a massive to locally foliated granodiorite containing 10% of mafic minerals, which intruded and stitches the Opinaca-La Grande contact (Bandyayera and Lacoste, 2009; Bandyayera et al., 2010). The Janin suite, in the Opinaca Subprovince, is composed of several units from pegmatite, tonalite, granite to granodiorite with hornblende and biotite (Bandyayera and Fliszár, 2007; Bandyayera et al., 2010). In the vicinity of the Éléonore mine, syn- to late-tectonic intrusions and pegmatite dykes (2620-2603 Ma) intruded the La Grande Subprovince supracrustal rocks (Ravenelle et al., 2010; Dubé et al., 2011; Fontaine et al., 2015). One of those, the 2612±1 Ma Cheechoo intrusion (Fontaine et al., 2015) is located 15 km southeast of the Éléonore mine (Fig. 1). The Cheechoo intrusion contains pegmatite dykes, mafic schist enclaves and hosts gold mineralization at Cheechoo (Fig. 2) and Éléonore South properties (Sirios Inc, 2016; Azimut, 2017). The Éléonore gold mine (Goldcorp), Cheechoo (Sirios Resources), Moni, JT (Azimut Exploration), Synee (Goldcorp) prospects and Sakami (Canada Strategic Metals) and Lac Menarik (Harfang Exploration) properties occur along a NW-trending corridor characterized by a strong metamorphic gradient, roughly subparallel to the Opinaca-La Grande boundary (Gauthier et al., 2007).

GEOLOGY OF THE CHEECHOO PROPERTY

The Cheechoo property straddles the transition zone between the La Grande Subprovince with the high-grade metasedimentary rocks of the Opinaca Subprovince (Fig. 1). The inferred contact, affected by open folds, is defined by the appearance of migmatite towards the northeast (Fig. 1). This is illustrated on the Cheechoo property by the preponderance of paragneissic rocks and migmatites (metatexites with local diatexites). Other lithologies include the Cheechoo intrusion, leucogranitic dykes and veins, banded iron formations, amphibolites and conglomerates (Fig. 1). The 10 km^2 Cheechoo intrusion has homogeneous, very low magnetic susceptibilities, with local high magnetic domains at its margins, potentially associated with the presence of iron-rich formation with skarn-like assemblages in the metasedimentary package. To the south, an E-trending kilometric-scale F_2 synform control the distribution of the aluminosilicate-bearing pelite, iron-rich formation (Low Formation) and amphibolites (Kasak Formation). The exploration activity is focused on its western (FD and JT showings), southern (Moni and Contact trends) and eastern edges (Cheechoo showings; Fig. 1). Detailed mapping of the main stripping area (Fig. 2 and 3) and of the 6-9 trench (Fig. 4) depicts the key geological features of the auriferous system that is developed within or at the margins of the Cheechoo intrusion (Figs. 2, 3 and 4).

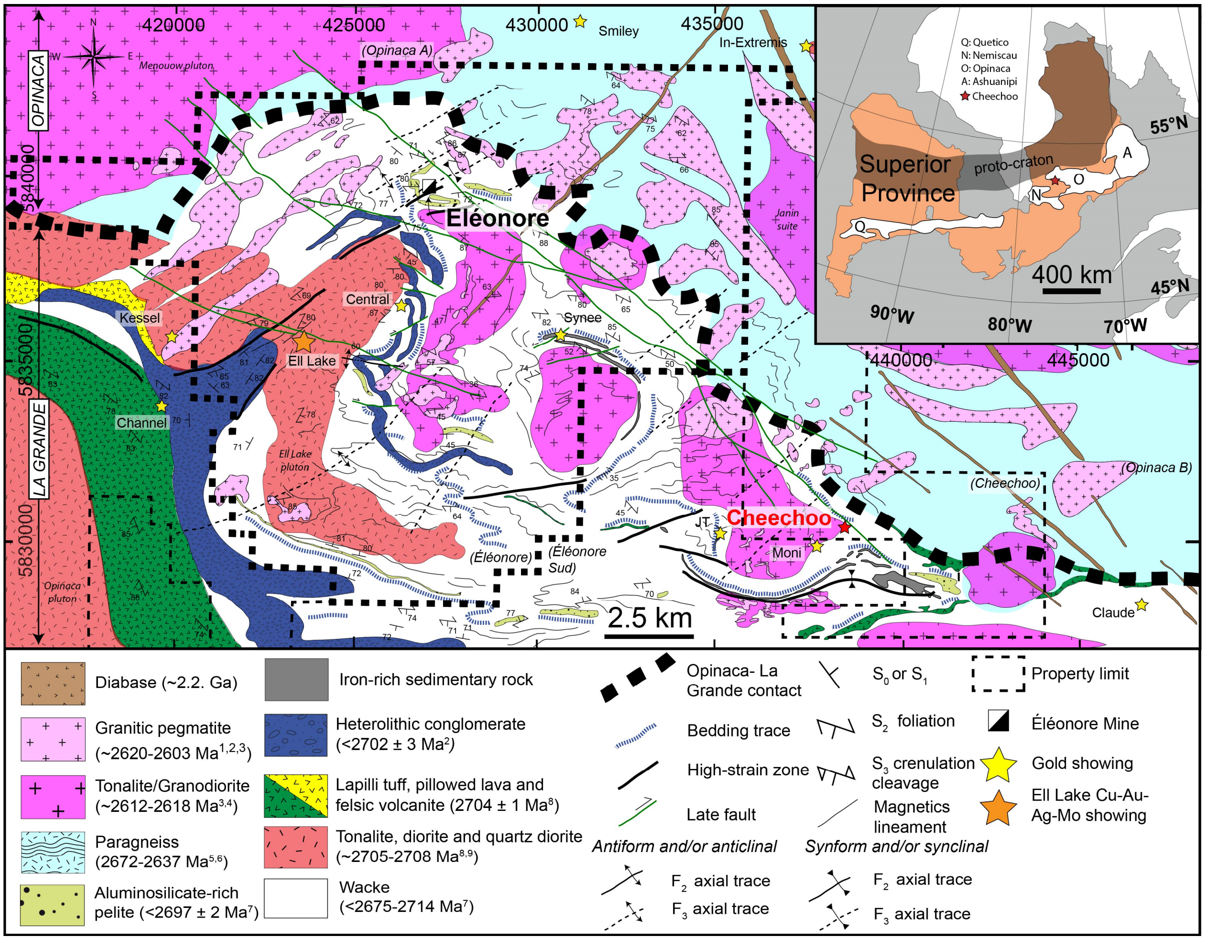

Figure 1: Simplified geological map of the Éléonore property and adjacent properties, modified after Fontaine et al. (2017a). Source of geochronological data: 1: (Dubé et al., 2011); 2: (Ravenelle et al., 2010); 3: (Fontaine et al., 2015); 4: (Goutier et al., 2000); 5: (David et al., 2010); 6: (Morfin et al., 2013); 7: McNicoll V., unpublished; 8: (Bandyayera and Fliszár, 2007); 9: David, J., 2005, unpublished. Proto-craton from (Percival et al., 1994). Coordinates NAD83, UTM, 18N zone.

The main stripped area exposes two distinct domains of the Cheechoo intrusion and two E-trending sections through its margins (Fig. 2). The mineral assemblage of the intrusion is characterized by feldspar phenocrysts and biotite porphyroblasts in a matrix of quartz, feldspars, biotite, amphibole and local traces of diopside and actinolite (Fig. 5A and B). The intrusion is characterized by a massive and a sacharoidal domain (Fig. 5A), and a more restricted highly foliated domain near its margins (25-30 m thick; Fig. 5B), which is associated with numerous leucogranitic pegmatite dykes (40-50%) that are generally sub-concordant to the foliation (Figs. 2 and 3). The foliation in the intrusion is mainly defined by elongated biotite porphyroblasts (Fig. 5B). In the western part of the main stripped area, highly-strained mafic schists occur as enclaves in the Cheechoo intrusion (Fig. 5C). Those mafic schist units are dismembered and cut by NE-trending pegmatite dykes (Fig. 5C). To the east, the paragneissic wacke, near the intrusion margins, is characterized by randomly-oriented amphibole porphyroblasts and injected by multiple apophyses of the Cheechoo intrusion (Fig. 5D). Ptygmatitic folds are locally well-developed in a chloritized paragneissic wacke containing an average gold grade of 1.4 g/t Au over 17 m (Fig. 2). A sillimanite-bearing paragneiss occur directly to the east of the chloritized paragneiss and illustrates the more pelitic (aluminium-rich) nature of some the sedimentary units (Fig. 2).Turbiditic wacke locally showing normal graded bedding (Fig. 5E) occur to the east of the paragneissic wacke (polarity to the north) and contains locally dismembered decimetric garnet, biotite, amphibole and epidote layers. Those layers may correspond to a metamorphosed volcanoclastic rock or a skarn-like metamorphic and/or hydrothermal assemblage (Fig. 2). In those layers, amphibole and/or biotite porphyroblasts are oriented parallel to the main foliation while garnet crystals are randomly oriented, suggesting, for the latter, a late static recrystallization. The 6-9 trench is located to the northwest of the main stripped area and exposes a domain of the Cheechoo intrusion, pegmatite dykes, paragneiss and an auriferous vein network (Fig. 4). The contact between the intrusion and paragneiss is affected by E-trending isoclinal folds and injected by leucogranitic dykes and veins. The Cheechoo intrusion is strongly recrystallized with sacharoidal texture, and progressively foliated towards its margins. The foliation within the intrusion is generally subparallel to the contact with biotite-rich paragneissic rocks (stereonet A on Fig. 4). This feature contrasts with NE-striking magnetic lineaments in the core of the intrusion, which are sub-parallel to regional F_3 axial planes (Fig. 1). These paragneiss contain decimetric amphiboles-rich layers and chaotic quartz-feldspar veinlets in association with pegmatite dykes (Fig. 4). The latter are composed of highly variable amount of quartz, feldspar (plagioclase, microcline) and to a lesser extent of biotite, apatite, tourmaline and chlorite (Fig. 5F). A zonation is sometimes present (e.g., facies dominated by quartz in the core and by feldspars at margins). The high variability of mineral assemblages and proportions, enrichment in volatiles elements (e.g. boron, and phosphorus) and the presence of miarolitic cavities suggest that these complex pegmatites are possibly at the magmatic-hydrothermal transition (exsolution of magmatic volatile phases from silicate melt).

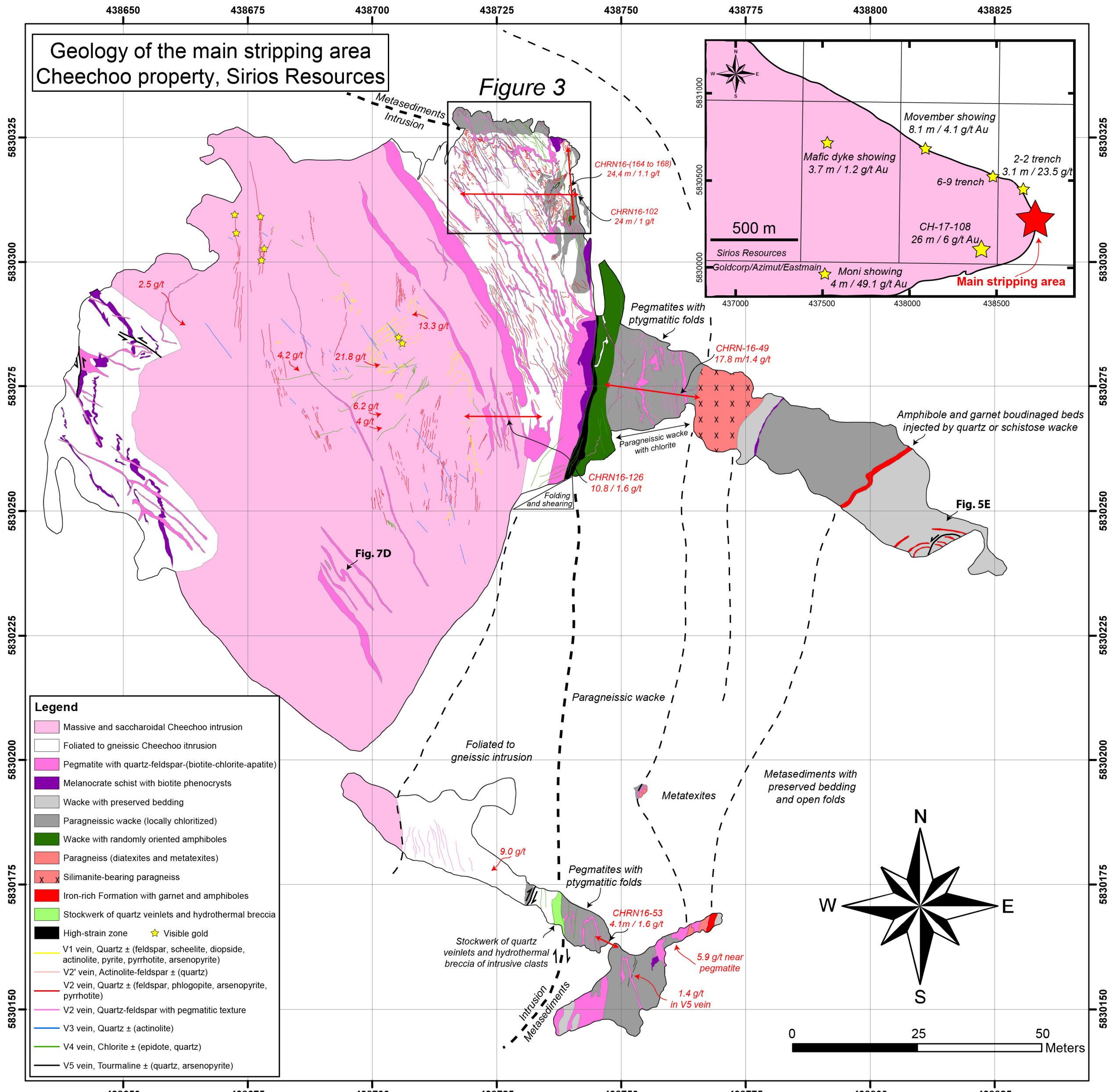

Figure 2: Geology of the main stripped area (modified from Pelletier and Gauthier, 2016, unpublished data). 2000 meters of channel sampling indicate an average grade of 0.4 g/t Au. The northeastern part of the Cheechoo intrusion is characterized by an increase of ductile strain and in abundance of veins and pegmatite dykes (see figure 3 for details). Coordinates NAD83, UTM, 18N zone.

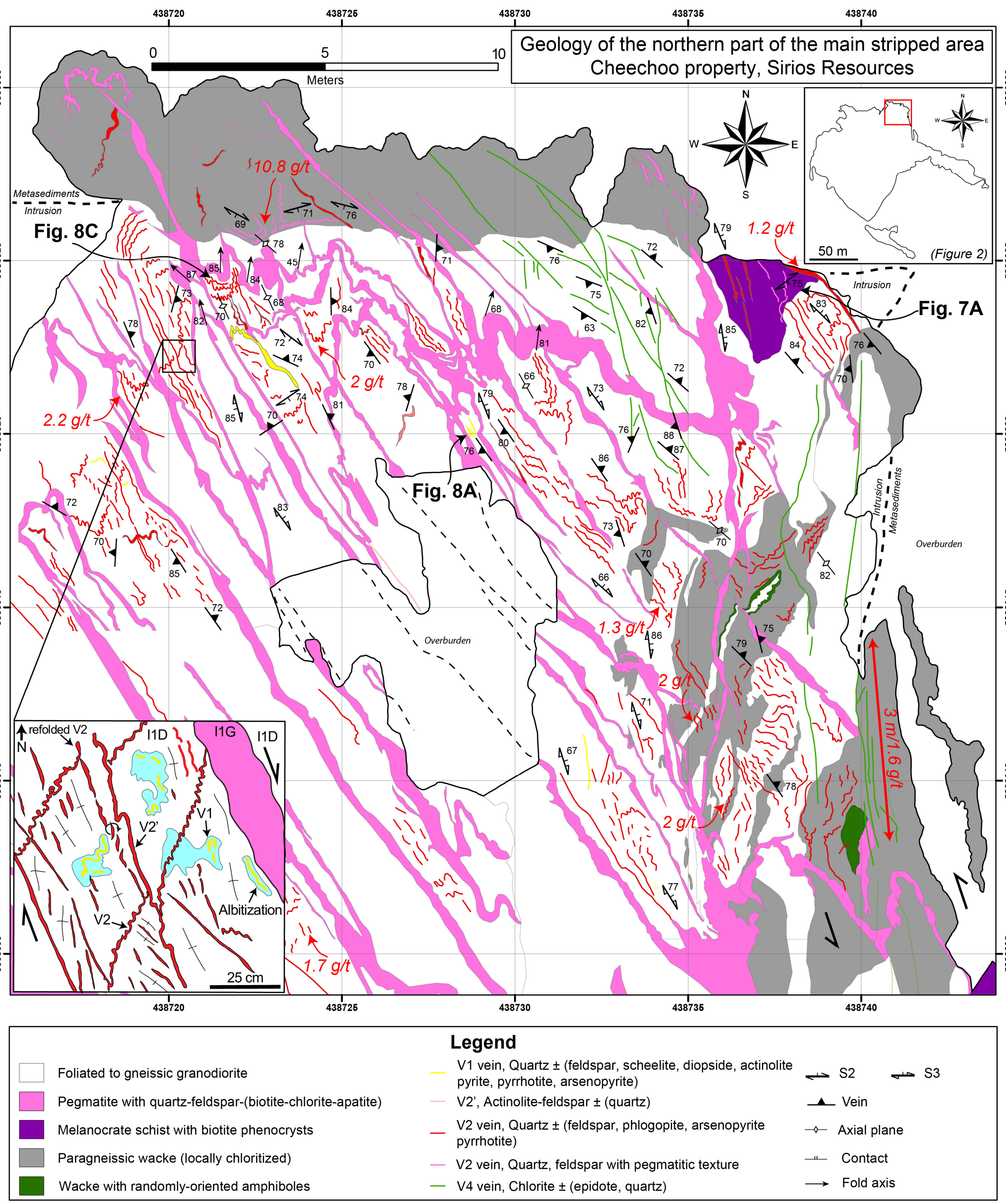

Figure 3: Detailed geological map of the northern part of the main stripped area. The vein network is spatially associated with pegmatite dykes and veins and tonalite apophyses. The E-striking S_2 fabric and pegmatite dykes are strongly transposed into the S_3 foliation, and affected by F_3 folds and high-strain zones. To the east, a pegmatite dyke, intruding the paragneissic wacke, is affected by an asymmetric s-shaped folding suggesting an anticlockwise rotation, compatible with a sinistral shear component along the high-strain zone. Coordinates NAD83, UTM, 18N zone.

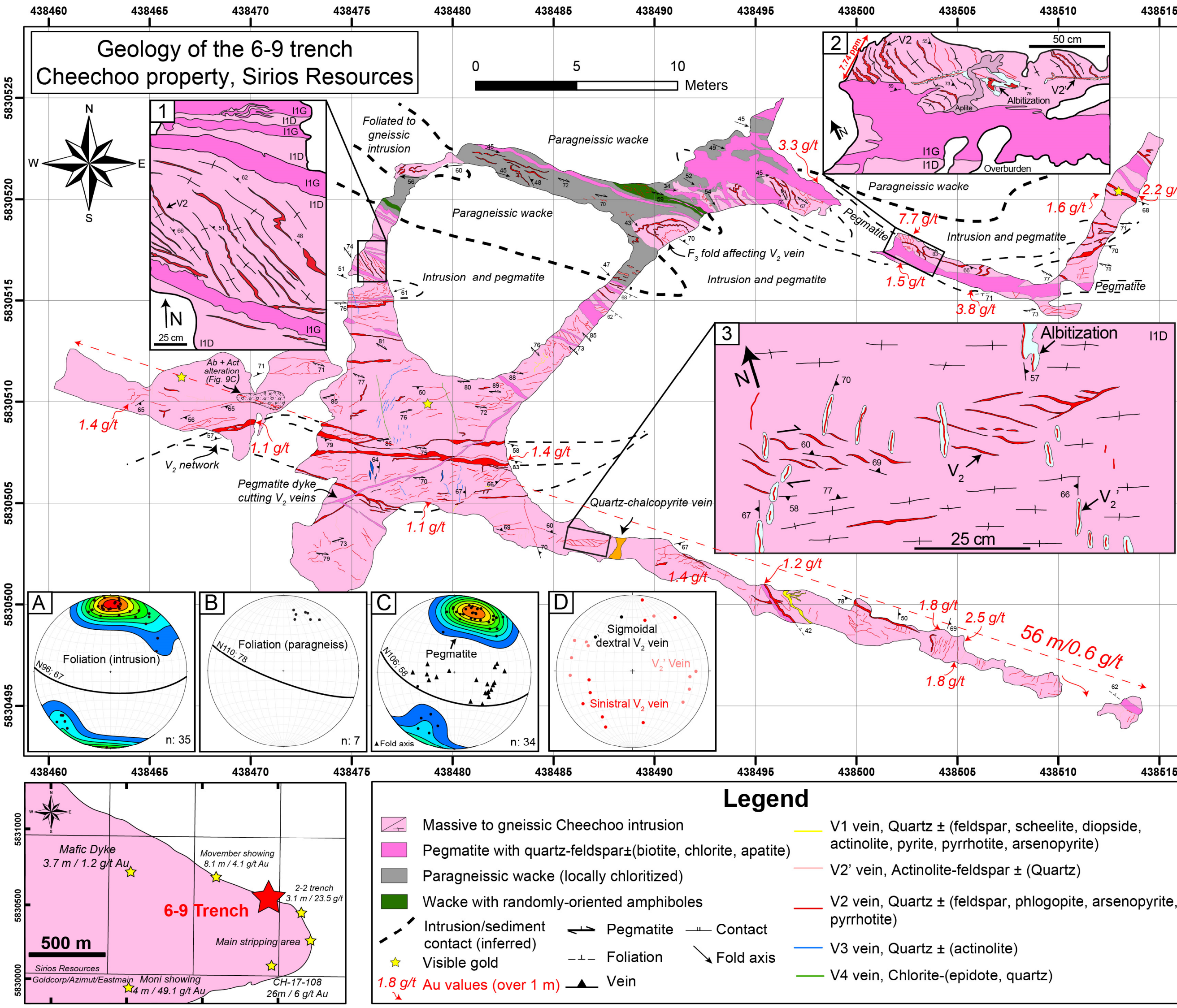

Figure 4: Geology of the 6-9 trench with detailed sketches and stereographic projections of key structures and vein sets. 1: V_2 vein are emplaced during increment of dextral shear occurring between two pegmatite dykes. 2: V_2 vein network (7.74 g/t over 1 m) intimately associated with a pegmatite dyke emplaced at the margins of the Cheechoo intrusion. 3: En-echelon V_2 vein network compatible with E-, NE-striking dextral shear component associated with discrete high-strain zones. Stereographic projections with Kamb contours (Kamb, 1959) of foliation within A) the Cheechoo intrusion, B) and the paragneiss wacke and orientations of C), pegmatite dykes and D) V_2 vein network (D). Coordinates NAD83, UTM, 18N zone.

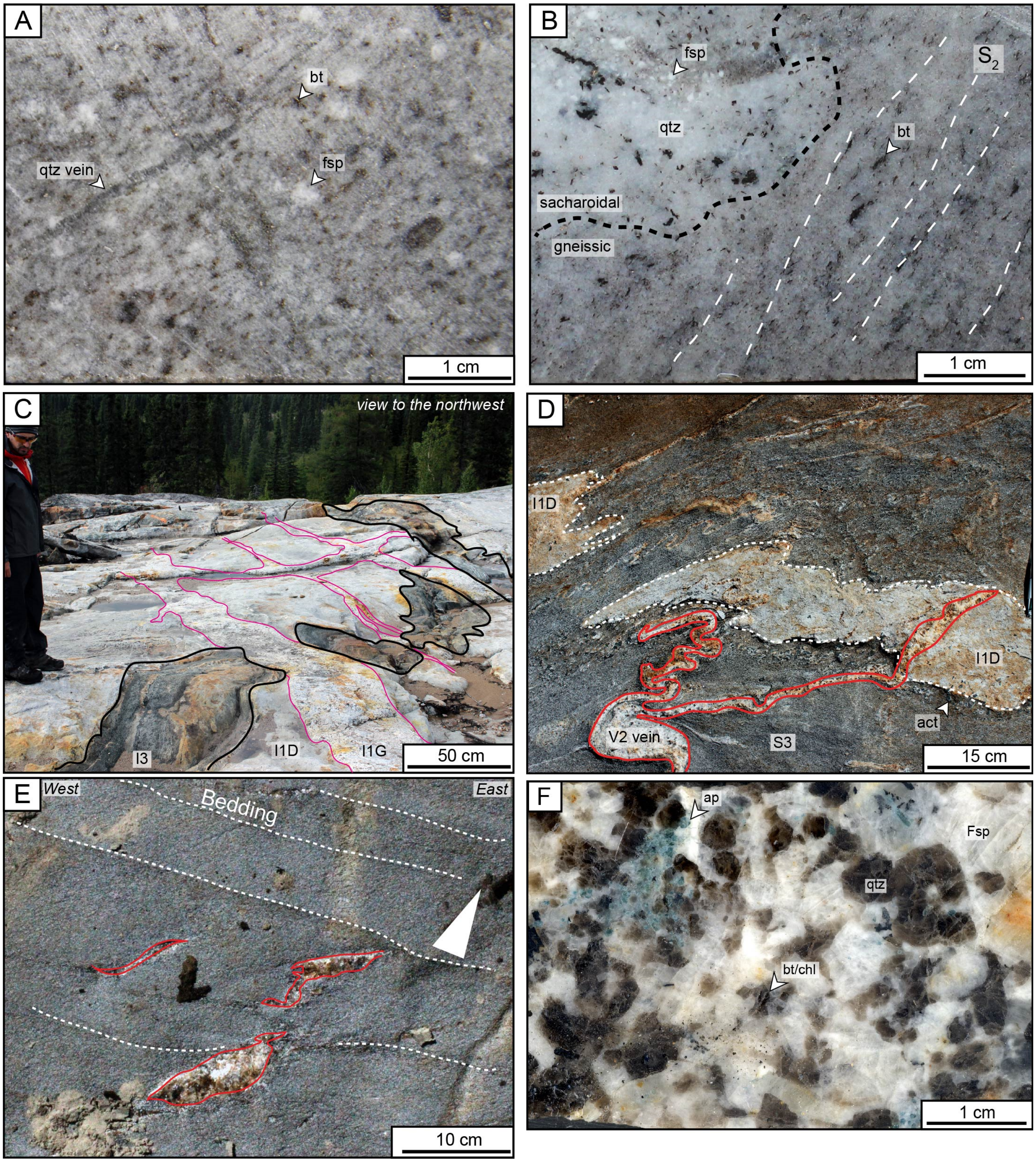

Figure 5: Lithologies of the Cheechoo property. A) Porphyritic facies of the Cheechoo intrusion with biotite and feldspar phenocrysts. B) Weakly foliated intrusion with sacharoidal texture. C) Mafic schist enclaves cut by a pegmatite swarm within the Cheechoo intrusion (main stripped area). D) Cheechoo apophyses within a paragneissic wacke with randomly-oriented amphiboles cut by an auriferous pegmatitic vein. E) Wacke with locally preserved bedding indicateing a polarity to the north and sigmoidal quartz-feldspar sigmoidal vein suggesting an apparent sinistral sense of shear (main stripped area). F) Pegmatite dyke composed of quartz, feldspar, chlorite, biotite and apatite (6-9 trench; CHE-17-06).

GEOCHEMISTRY

In order to constrain the geochemical signature of the intrusion and hydrothermal alteration associated with the auriferous vein network, several samples were collected from drill holes and trenches (n: 10). Samples with loss on ignition < 1 wt %, sulfur content < 0.5 wt %, CO_2 < 0.5 wt % and without any petrographic evidence of mineralization or veining, have been classified as less altered samples (Table 1). The geochemistry of the Cheechoo intrusion is compared to other intrusions of the area: i) leucogranite samples from the Opinaca Subprovince (OP-Leucogranites), ii) granite samples from the Vieux Comptoir magmatic suite, iii) granodiorite to granite samples from the Janin suite, iv) granite samples from the Rotis pluton, v) average wacke composition of the Opinaca Subprovince and from the Low Formation, vi) pegmatites and vii) mafic schist enclaves (Fig. 6). Feldspar compositions of the Cheechoo intrusion, analyzed by electron microprobe, are also plotted on the normative Ab-An-Or diagram in order to compare with calculated Cross, Iddings Pirsson and Washington (CIPW) norm (Fig. 6B).

Cheechoo intrusion

On the QAP diagram, Cheechoo samples plot on the granodioritic, quartz monzodioritic and quartz-dioritic fields (Fig. 6A). Average Opinaca wacke plots on the granodioritic field while Opinaca leucogranites are concentrated in the granite field and some of them are granodioritic (Fig. 6A). On the feldspar normative plot (Fig. 6B), Cheechoo samples plot on the trondhjemitic field, coherent with feldspar microprobe analysis (Ab_{94} to Ab_{80}). Opinaca leucogranites, Rotis, Janin and Vieux Comptoir, plot on the granite field with a high orthose content (Fig. 6B). The majority of Opinaca leucogranites plot in granitic field with some samples in the trondhjemite and granodiorite fields. All samples from Cheechoo intrusion plot within the granodiorite field on the SiO_2 versus Zr/TiO_2 diagram, with narrow SiO_2 range (67.9 to 70.6 wt %) and a low Zr content (generally < 55 ppm) whereas the Opinaca leucogranites have granite or alkaline granite compositions (Fig. 6C). The Cheechoo samples contrast with TTG such as the Janin suite, or the Rotis pluton based on low contents of Ni (< 15 ppm), Cr (< 30 ppm) and MgO contents (generally < 1.5 wt %) of the Cheechoo samples. However, the A/CNK versus A/NK diagram indicates that Cheechoo, Janin and Rotis generally share common metaluminous signatures that differ with the peraluminous nature (mainly I-type) of the Vieux Comptoir suite and Opinaca leucogranites (Fig. 6D). On the $[Gd/Lu]_N$ versus $[Hf/Sm]_N$ diagram (normalization to the C1 chondrite), Opinaca leucogranites, Cheechoo and associated pegmatites shared a common potential differentiation trend and source(s) such as metagreywacke and/or TTG, and the influence of assimilation, fractionation and contamination (AFC) during ascent and emplacement (Fig. 6E). On the A/CNK-Na_2O/K_2O-FMSB ternary diagram, the Cheechoo samples plot between the TTG and 2-micas granite fields (Fig. 6F). Cheechoo samples on the TTG field are characterized by high Na_2O contents (Fig. 6F). Cheechoo samples have C1-normalized REE patterns lower than average Opinaca leucogranites, and average Opinaca wacke (Fig 6G). However Cheechoo samples have similarities with some leucogranites (group 3) defined by Morfin et al. (2014). Similarly to this group of leucogranites, Cheechoo samples have a moderate slope (La/Yb_N =5.6) and display a small positive Eu anomaly with Eu/Eu* between 1.1 and 2.3 (where $Eu/Eu^* = Eu_N/(Sm_N \cdot Tb_N)^{1/2}$). This group of leucogranites is interpreted as cumulate of k-feldspars formed from less fractionated melts compared to the others leucogranites of the Opinaca Subprovince (Morfin et al., 2014). This is supported by a low Rb/Sr ratio, a feature shared with the Cheechoo intrusion (Table 1).

Pegmatite dykes

Pegmatite dykes have a granitic composition with SiO_2 generally > 70 wt% and Zr/TiO_2 between 0.03 and 0.25, high K_2O (> 3.5 wt %), low CaO (< 1.2 wt %), low MgO (< 0.5 wt %), low to moderate Al_2O_3 (< 15 wt %). One pegmatite sample has very high SiO_2 content (> 80 wt %) in association with moderate P_2O_5 content (0.51 wt %), coherent with the presence of apatite. The total REE contents are elevated for the apatite-rich pegmatite on the 6-9 trench (∑REE = 51.3 ppm) and low in the pegmatite containing chlorite and phlogopite (∑REE = 6.8 ppm).

Mafic schists

Mafic schists have moderate SiO_2 content (55.7 wt %), high MgO (> 10 wt %), high CaO (> 5 wt %), low Al_2O_3 (< 13 wt %), moderate Na_2O (< 5 wt %), low to moderate K_2O (< 1.5 wt %), low MgO (> 8 wt %) and low TiO_2 (< 0.6 wt %). Interestingly, mafic schists are characterized by high As (> 1500 ppm), Au (80 ppb), Cr (> 300 ppm) V contents (>130 ppm). They have also high La/Yb_N ratio (10.7), high LILE (Cs, Rb, Sr and Ba) and low HFSE elements contents (Nb, Hf, Zr, Th and U). Mafic schist enclaves plot on the gabbro-diorite field on the Zr/TiO_2 versus SiO_2 diagram (Fig. 6C). The Hf/Sm_N and Gd/Lu_N values for the mafic schist plot closed to the values for wacke of the Low formation and within the Opinaca Subprovince (Fig. 6E). These geochemical features (Table 1), along with the presence of biotite-phlogopite, k-feldspar and amphiboles, share similarities with calc-alkaline lamprophyres (Rock, 1987; Wyman and Kerrich, 1993; Taylor et al., 1994) and with the 2b group of Baie-James magnesian swarm, defined by Vigneau (2011).

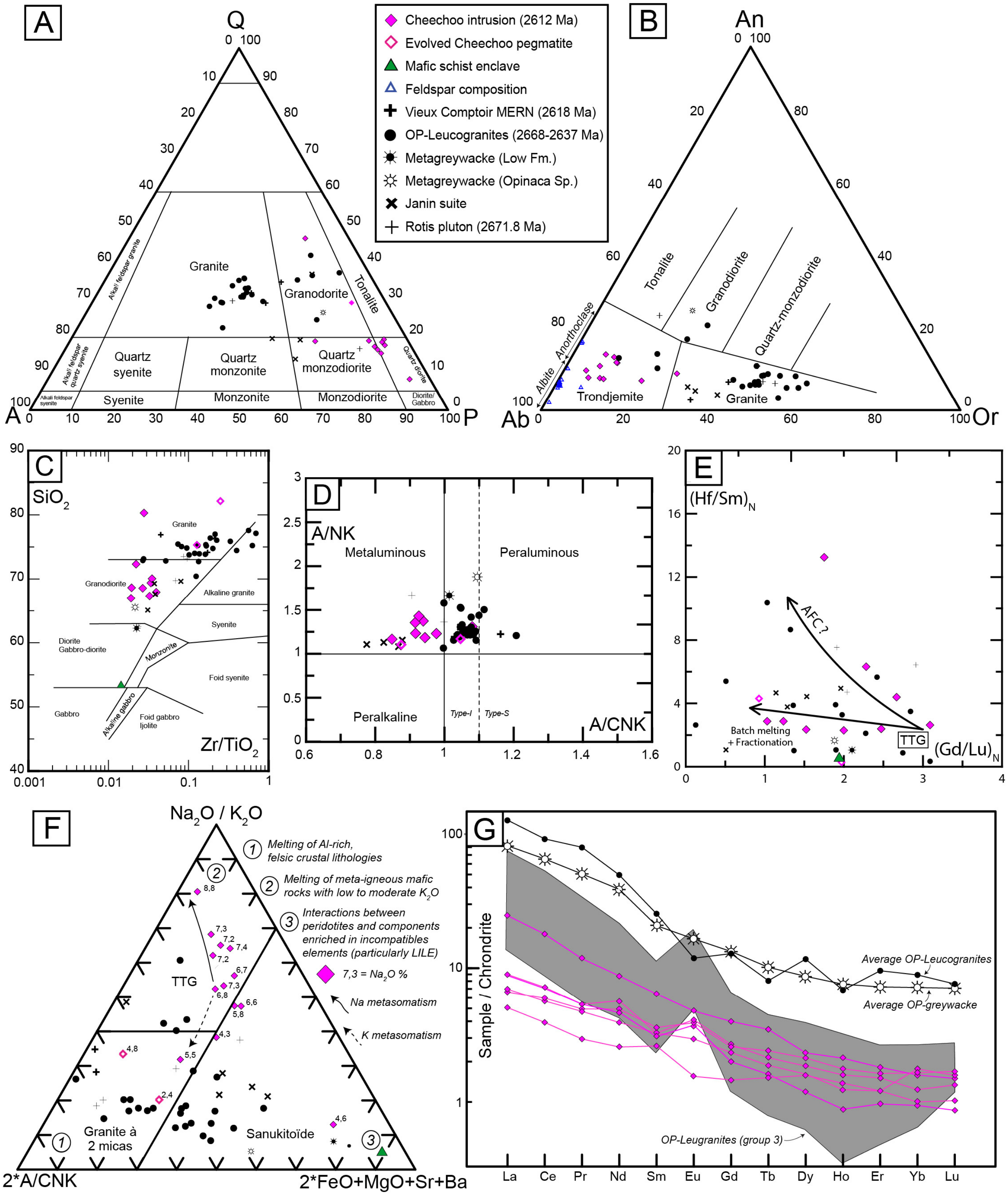

Figure 6: Geochemical features of the Cheechoo intrusion compared to other intrusions in the area. A) Quartz-alkali feldspar-plagioclase diagram by Streckeisen (1976). B) Feldspar normative of Albite-Anorthite-Orthose diagram from O'connor (1965); C) SiO_2 vs Zr/TiO_2 (Winchester and Floyd, 1977). D) Shand index plot with A/CNK=Al_2O_3/(CaO+Na_2O+K_2O), A/NK= Al_2O_3/(Na_2O+K_2O), in moles (Maniar and Piccoli, 1989); E) $[Gd/Lu]_N$ versus $[Hf/Sm]_N$ diagram (normalized to the C1 chondrite) inspired from Galley and Lafrance (2014) with C1 chondrite values from McDonough and Sun (1995) and TTG values from Laurent et al. (2014). F) A/CNK–Na_2O/K_2O-(FeO+MgO+Sr+Ba) ternary diagram from Laurent et al. (2014). G) REE patterns (normalized to the C1 chondrite) for the Cheechoo intrusion, average Opinaca wacke and Opinaca leucogranites (group 3 defined by Morfin et al., 2014).

Location		**Cheechoo property (Sirios Resources), Eeyou Itchee Baie-James, Québec, Canada**								
Sample		**Less altered**		**Altered**		**CHE-17-03**	**Cryptic Na**	**CHE-17-06**	**CHE-14-03**	**CHE-17-05**
Rock type		**Cheechoo**		**Cheechoo**		**V1 vein**	**Cheechoo**	**Pegmatite**	**Pegmatite**	**Mafic schist**
Oxides / wt.%	D.L.	n: 2	SD	n: 8	SD		n: 2			n: 2
SiO_2	0,01	68,64	0,83	69,88	4,33	72,31	68,28	82,15	75,31	53,52
TiO_2	0,001	0,13	0,02	0,14	0,03	0,12	0,13	0,01	0,03	0,56
Al_2O_3	0,01	18,08	1,27	16,19	2,50	14,85	17,71	8,91	14,15	12,05
Fe_2O_3	0,01	0,08	0,08	0,14	0,17	< D.L.	< D.L.	< D.L.	0,66	0,76
FeO	0,1	0,85	0,47	1,41	0,62	2,30	1,20	0,70	< D.L.	7,00
MnO	0,001	0,02	0,01	0,03	0,03	0,03	0,02	0,02	0,01	0,21
MgO	0,01	0,58	0,24	1,03	0,44	0,63	0,67	0,06	0,26	10,33
CaO	0,01	2,23	0,25	1,69	0,54	1,73	2,17	1,16	0,78	7,13
Na_2O	0,01	7,62	1,05	6,76	1,35	5,83	8,10	2,44	4,80	3,63
K_2O	0,01	1,09	0,35	1,48	0,87	1,27	0,84	3,75	3,89	1,80
CO_2	0,01	0,12	0,18	0,39	0,60	0,05	0,19	< D.L.	0,26	0,02
LOI		0,37	0,31	0,80	0,78	0,34	0,40	0,27	0,48	1,25
S	0,01	0,14	0,19	0,24	0,10	0,40	0,08	< D.L.	0,03	0,03
Total		99,94		100,19		99,46	99,68	99,46	100,63	98,24
Trace elements / ppm										
Au	0,005	0,02	0,01	0,29	0,37	7,25	0,30	0,03	0,29	0,08
As	0,1	138,25	175,01	513,88	410,38	1700,00	1220,00	21,30	41,00	2405,00
Bi	0,02	0,09	0,10	0,34	0,68	76,30	< D.L.	0,41	1,73	0,08
Sb	0,02	0,11	0,01	0,42	0,40	0,54	< D.L.	0,08	0,15	0,13
Se	0,1	0,18	0,19	0,40	0,18	0,70	< D.L.	< D.L.	0,50	< D.L.
Te	0,02	0,02	0,03	0,02	0,04	0,49	< D.L.	< D.L.	< D.L.	< D.L.
W	0,5	6,27	7,13	3,66	2,60	1440,00	3,30	< D.L.	5,00	5,60
Sn	1	2,25	2,47	1,00	1,23	< D.L.	2,25	< D.L.	< D.L.	7,00
Mo	2	0,75	0,35	3,66	2,60	< D.L.	0,75	< D.L.	< D.L.	< D.L.
Cs	0,1	2,68	1,78	5,26	4,31	5,10	1,00	4,20	19,80	61,80
Rb	1	30,50	17,04	44,63	24,99	38,00	19,00	91,00	187,00	178,00
Sr	2	431,50	55,08	349,75	74,27	327,00	519,00	126,00	139,00	272,50
Ba	2	610,00	456,29	442,75	367,30	219,00	361,00	486,00	371,00	166,50
Y	0,5	3,30	1,96	2,36	1,31	3,30	1,80	32,10	4,00	15,90
Zr	1	47,33	4,73	40,75	8,447	27,00	42,00	20,00	42,00	81,00
Hf	0,1	1,50	0,15	1,18	0,46	0,80	1,20	0,70	1,20	2,20
Nb	0,2	4,35	4,30	1,46	2,67	0,70	0,50	0,50	< D.L.	4,60
Ta	0,01	7,66	8,20	2,08	5,31	0,18	0,12	1,69	0,90	1,34
Th	0,05	0,66	0,26	0,33	0,26	0,16	0,14	2,88	6,30	3,90
U	0,1	0,68	0,50	0,36	0,26	2,29	1,01	0,88	18,60	1,65
V	5	20,33	10,97	14,25	12,32	20,00	23,00	< D.L.	< D.L.	140,00
Ni	1	9,00	1,00	10,75	2,38	15,00	12,00	2,00	< D.L.	99,00
Cr	0,5	18,00	10,58	26,25	18,47	27,00	29,00	23,00	< D.L.	404,00
REE / ppm										
La	0,05	1,92	0,17	1,83	0,54	5,86	2,87	4,80	1,20	23,20
Ce	0,05	4,72	0,55	3,64	1,00	11,00	6,17	14,30	2,40	51,10
Pr	0,01	0,64	0,16	0,44	0,12	1,12	0,66	2,03	0,28	6,38
Nd	0,05	2,64	0,71	1,98	0,60	4,09	2,48	8,68	1,20	25,70
Sm	0,01	0,77	0,34	0,50	0,17	0,98	0,58	3,58	0,40	5,08
Eu	0,005	0,21	0,03	0,19	0,05	0,28	0,23	0,25	0,09	0,69
Gd	0,01	0,61	0,27	0,42	0,15	0,82	0,51	4,72	0,30	3,55
Tb	0,01	0,09	0,06	0,06	0,02	0,13	0,07	0,93	< 0.1	0,52
Dy	0,01	0,59	0,34	0,36	0,14	0,59	0,37	5,76	0,40	2,94
Ho	0,01	0,10	0,08	0,06	0,02	0,12	0,07	0,98	< 0.1	0,53
Er	0,01	0,34	0,20	0,19	0,09	0,30	0,22	2,56	0,20	1,49
Tm	0,005	0,05	0,04	0,03	0,01	0,04	0,03	0,35	< 0.05	0,23
Yb	0,01	0,37	0,25	0,16	0,10	0,27	0,22	2,09	0,30	1,55
Lu	0,002	0,06	0,04	0,03	0,02	0,04	0,03	0,30	0,04	0,23

Table 1: Major element of Cheechoo whole-rock samples analyzed by FUS-ICP (SiO_2, TiO_2, Al_2O_3, Fe_2O_3, MnO, MgO, CaO, Na_2O, K_2O, CO_2, LOI, Ba, Zr and Sr) and TITR (FeO) and trace element analyzed by FUS-MS (Cs, Rb, Y, Hf, Nb, Ta, Th, U, V, W, Mo and Sn), AR-MS (As, Bi, Sb, Se and Te), FA-AA (Au), FA-GRA (Au if >5000ppb) and TD-MS (Cr and Ni). D.L.: detection limit.

STRUCTURAL GEOLOGY

Regional framework

The Cheechoo property is located a few kilometers south of the tectonic contact between the Opinaca and La Grande sub-provinces (Bandyayera et al., 2010; Ravenelle et al., 2010). Here, deformed high-grade metasedimentary rocks are ubiquitous (e.g. migmatites with ptygmatitic folds) and also similar to those described elsewhere in the area by Morfin et al. (2013). Within the Opinaca Subprovince, deformation commonly occur during granulite facies metamorphism and partial melting (Simard and Gosselin, 1999). The S_1 fabric is totally obliterated by the main phase of deformation and regional metamorphism although transposed S_0 is locally preserved in metatexites or inferred by variations in grain sizes and mineral proportions (Bandyayera et al., 2010; Morfin et al., 2013). The main S_2 fabric is a paragneissic fabric and/or migmatitic layering (Ravenelle et al., 2010). Leucocratic veins and dykes commonly strike parallel to the transposed bedding and some are asymmetrically folded (Morfin et al., 2013; Morfin et al., 2014), while others cut this fabric suggesting that migmatization occurred during and outlasted D_2 (Ravenelle et al., 2010). The generally subvertical S_2 fabric is defined by biotite or amphibole alignments, with mineral and stretching lineations plunging to the east or the west (Bandyayera et al., 2010). The Cheechoo study area is part of the structural domain 2 of Bandyayera et al. (2010), characterized by EW-striking transposed bedding subparallel to S_1 and S_2 foliation, except along F_2 fold hinges that generally plunging to the west (Bandyayera et al., 2010).

The E-striking S_2 fabric and compositional layering of paragneiss are locally refolded by doubly plunging folds forming an elongated dome-and-basin pattern (Ravenelle et al., 2010), as originally described by Remick (1977). This specific pattern is due to F_3 folds and/or local doming associated with diapiric emplacement of late-tectonic intrusions (Bandyayera and Fliszár, 2007; Ravenelle et al., 2010; Fontaine et al., 2017b). A S_3 crenulation cleavage and associated inclined small-scale folds, deforms the S_2 fabric and migmatitic layering (Bandyayera et al., 2010). As proposed by Bandyayera et al. (2010), late-tectonic intrusions (e.g. Rotis, Menouow plutons and Vieux Comptoir, Janin suites), also influenced the trend of the S_2 fabric with local concentric distribution, as illustrated in the vicinity of the Rotis pluton. Flanks of F_2 and/or F_3 folds are locally truncated by EW-striking subvertical high-strain zones, attributed to a D_4 event (Morfin et al., 2013). The regional pattern is coherent with a NS-oriented shortening (Morfin et al., 2013).

Planar fabrics

The margins of the Cheechoo intrusion are foliated to gneissic (Fig. 2), and characterized by elongated biotite porphyroblasts, commonly attributed to the sub-magmatic S_2 foliation (stereonet A on Fig. 7). The latter is commonly reoriented along the NW- to N-striking S_3 foliation (Fig. 3). On the main stripped area, the S_2 foliation is visible in the gneissic margins of the Cheechoo intrusion, spatially associated with the presence of sheeted pegmatite dykes (Figs. 7B and C). The S_3 foliation dips steeply to the E-NE (76°; n: 25; stereonet B on Fig. 7), similar to the S_2 foliation within the paragneiss and mafic schists, to the north of the main stripped area (stereonet on Fig. 7A). In the paragneissic wacke, the S_2 and S_3 foliations are characterized by EW-striking bedding-parallel foliation and NW-striking crenulation cleavage, respectively, (Fig. 7A). The S_3 crenulation cleavage is also present within mafic schist enclaves (Fig. 2). On the 6-9 trench, the E-striking moderately-dipping S_2 foliation is present within the intrusion (stereonet A on Fig. 4), while the dip of the S_2 foliation is steeper in the paragneissic wacke (stereonet B on Fig. 4). Pegmatite dyke commonly oriented sub-parallel to intrusion margins (stereonets C on Figs. 4 and 7).

Folds

At least two generations of folds can be mapped in the Cheechoo intrusion. The most common type is F_3 fold affecting the S_2 foliation and pegmatite dykes (Fig. 7B and D). F_3 microfolds and axial-planar S_3 crenulation cleavage are also developed in the paragneissic rocks (Fig. 7A). F_3 folds are open, tight to isoclinal with strong asymmetries suggesting a close link with high-strain zone during late-D_2 to D_3. F_3 fold axes are often curvilinear, locally shallow plunging to the east or to the west (stereonet D on Fig. 7), a feature also observed in the Opinaca Subprovince (Ravenelle et al., 2010). Refolded planes (S_2 foliation, vein and pegmatite dykes) in F_3 folds suggest the presence of F_2 folds. Earlier folding (F_1 and/or F_2) can be inferred based on the geometry of mafic schist enclaves and the local refolded pegmatite dykes (Fig. 2). In the paragneissic rocks, F_2 folds with S_2 axial planar are locally identified.

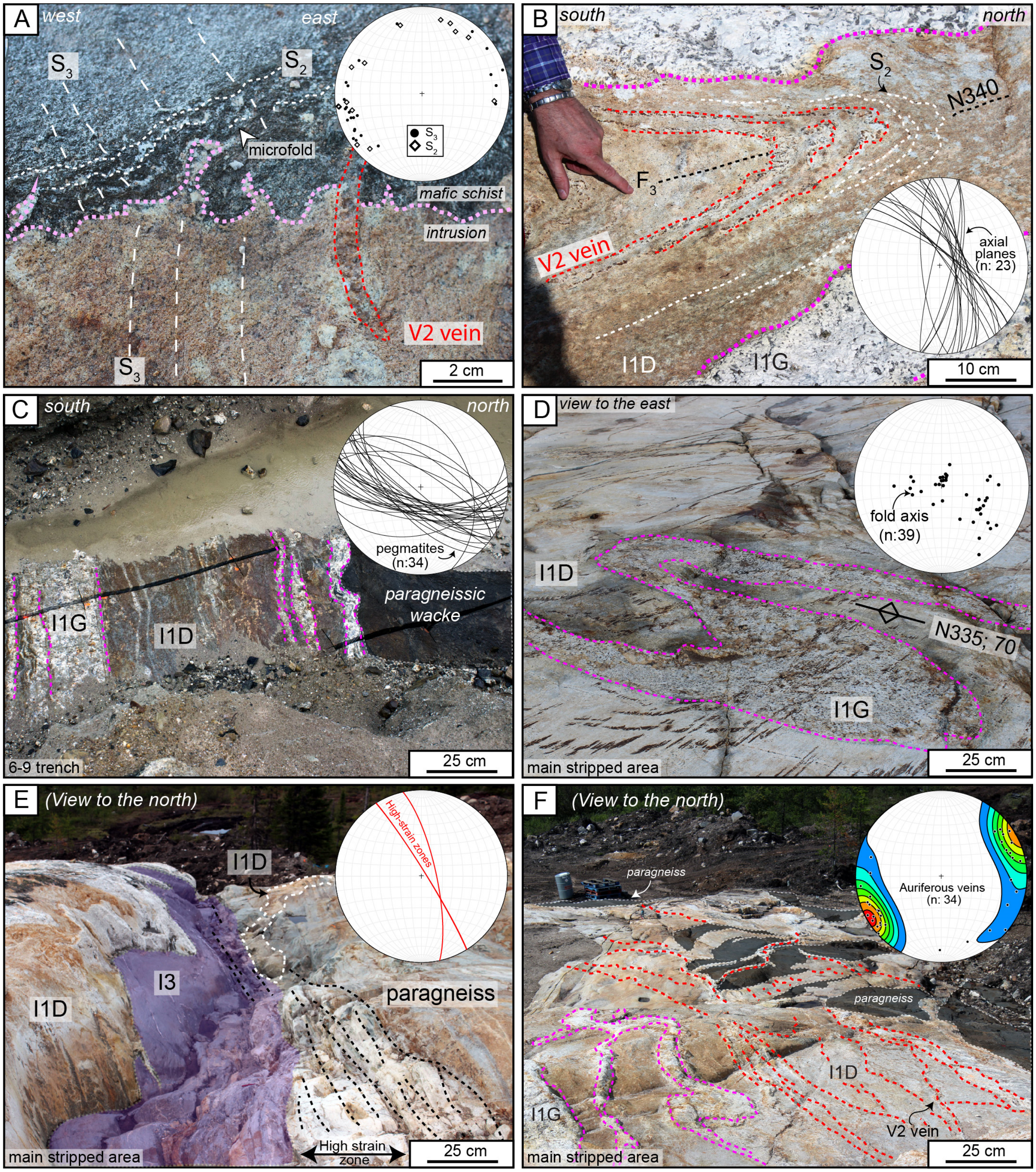

Figure 7: Selected structural features. A) NW-striking S_3 foliation in the Cheechoo intrusion and E-trending S_2 foliation crenulated by S_3; B) S_2 and V_2 vein folded by N-trending F_3 folds with pegmatite dykes oriented along the F_3 axial plane; C) E-trending pegmatite dykes (I1G) sub-parallel to the contact between wacke and Cheechoo intrusion (6-9 trench); D) Asymmetric F_3 isoclinal fold deforming a pegmatite within the Cheechoo intrusion; E) High-strain zone in paragneissic rocks at the contact with a foliated mafic dyke (I3) and the Cheechoo intrusion (I1D) ; F) Contact between paragneissic wacke and the intrusion (I1D) showing presence of tonalite apophyses and/or dykes, pegmatites and a NNE-trending pegmatitic V_2 vein network. Stereographic projections: A) S_2 foliation (black diamonds) and S_3 black circles), B) S_3 and F_3 axial planes, C) pegmatites orientations, D) F_3 fold axis and E) high-strain zones at the intrusion margins F) V_2 vein network with Kamb contours (Kamb, 1959).

High-strain zones and late brittle faults and breccia

A late-D_2 to D_3 N-striking high-strain zone is developed in the paragneissic rocks at the margins of the intrusion (Figs. 2 and stereonet E on Fig. 7). High-strain zones locally cut tonalite apophyses (Fig. 7E) and affect pegmatite dykes (Fig. 3) and V_2 vein (stereonet F on Fig. 7). On the main stripped area (Fig. 3), these high-strain zones are parallel with the S_3 foliation in the paragneiss suggesting that they may have developed during late-D_2 to D_3, in response to competency contrast and strain partitioning between the stiff Cheechoo intrusion and softer surrounding paragneiss. A late D_4 breccia is superimposed on N-striking high-strain zones (Fig. 2). The breccia is composed of angular centimetric fragments of bleached intrusion and of a veinlet stockwork (V_4) composed of chlorite ± (epidote, quartz) with chlorite, epidote and feldspar narrow alteration zones. These features are similar to the late (post-ore) NW-striking regional fault, as described at the Éléonore gold mine (Ravenelle, 2013; Fontaine et al., 2015).

GOLD MINERALIZATION AND HYDROTHERMAL ALTERATION

The vein network of the Cheechoo property is composed of various types of auriferous veins including sheeted extensional, en-echelon quartz-dominated veins, as well as pegmatitic quartz-feldspar veins (Fig. 8A). Mainly occurring within the intrusion, but also in the surrounding paragneissic rocks, the vein network is commonly 40 to 50 meters wide and, at least, one hundred meters long (Fig. 2, 3 and 4). The vein density increases (from 15 to 50% of the rock volume) towards intrusion margins and with the occurrence of pegmatite dykes, tonalite apophyses and mafic schist (Fig. 2). The gold grade is controlled by the presence of sulphides (particularly arsenopyrite), the density of veins, and deformation gradients. The vein types (V_1, V_2, V_2', V_3, V_4 and V_5) is essentially based on crosscutting relationships and is not related to the nomenclature of deformation events. The early V_1 auriferous vein network (about 5% of the vein network) is composed of millimetric to centimetric veins characterized by quartz, feldspar and minor amounts of diopside, actinolite and scheelite in association with pyrite, pyrrhotite, arsenopyrite and local visible gold (Figs. 8A and B). Veins are generally dismembered, with diopside, actinolite, albite-rich centimetric halos (Fig. 8A). Those veins are mainly perpendicular or at high-angle with the margins of the Cheechoo intrusion (Fig. 2). V_2 veins (about 70% of the vein network) cut the V_1 vein network (Fig. 3) and are composed of quartz, feldspar, phlogopite, arsenopyrite and pyrrhotite (Fig. 8C). V_2 veins are oriented subparallel or at low-angle with the intrusion margins (Fig. 2) and form a sheeted vein array (Fig. 8D). For instance, in the southern part of the 6-9 trench, the auriferous en-echelon V_2 vein network is oriented at low-angle with the contact between the paragneiss and the intrusion, and is interpreted to represent ENE-trending dextral shear component associated with discrete high-strain zones (stereonet D on Fig. 4). V_2' veins (about 15% of the vein network) are composed of quartz ± feldspar and characterized by actinolite and feldspar-rich selvages (Fig. 4, inset 3). In all of those veins, feldspar is commonly interstitial to quartz grains (Figs. 8A and C), like those of some auriferous pegmatitic quartz-feldspar veins hosted by the Cheechoo tonalite (Moni showing) or by paragneiss at the Éléonore gold mine. Locally, pegmatites laterally evolve into V_2 and V_2' veins while some pegmatite dykes cut veins, suggesting that some of them may be contemporaneous (Figs. 2 and 3). V_3 are extensional veins (roughly 10% of the vein network) composed of quartz, actinolite, feldspar, (Fig. 8F). Those veins are N-striking on the 6-9 trench (Fig. 4) and NNE-striking on the main stripped area (Fig. 2). On the 6-9 trench, V_3 veins are oriented perpendicular to the intrusion margins and become progressively transposed sub-parallel to the contact towards the NNE, where they are also affected by F_3 folds (Fig. 4). In contrast, on the main stripped area, the V_3 veins are NNW-striking, subparallel to the intrusion margins (Fig. 2). Late V_4 are commonly barren. They are composed of chlorite ± (epidote, quartz) and oriented to the N/NNW in the northeastern part of the main stripped area (Fig. 2). V_4 veins locally contain pyrite and visible gold in association with chlorite. V_5 veins are located 40 m west of the intrusion margins in chloritized paragneiss. These veins comprise tourmaline ± quartz, arsenopyrite (Fig. 2; 1.4 g/t Au) and are sigmoidal and sub-concordant to the foliation and dip moderately to the east (50-60°) supporting a syn-D_2 emplacement.

Hydrothermal alteration assemblages

Two main types of hydrothermal alteration are present in the Cheechoo intrusion: a decimetric to metric Na-rich hydrothermal zone (early-Au) and centimetric K-Mg rich replacement zones/bands (syn-Au), preferentially located along V_2 vein selvages (Figs. 8A and D). A more restricted, calc-silicate and/or skarn-like alteration assemblage (e.g. actinolite, diopside and grossular) also occurs around some V_1 veins and also in the surrounding sedimentary rocks in the vicinity of the intrusion margins and its apophyses (Figs. 2 and 3). Less altered samples of the Cheechoo intrusion (Figs. 9A and B) are compared to those of the two types of hydrothermal alteration (Figs. 9C and D) and to a V_1 vein (Fig. 8A), using the method of Grant (1986). Less mobile elements such as Zr, TiO_2 and Al_2O_3 were used to build isocon lines (Fig. 10).

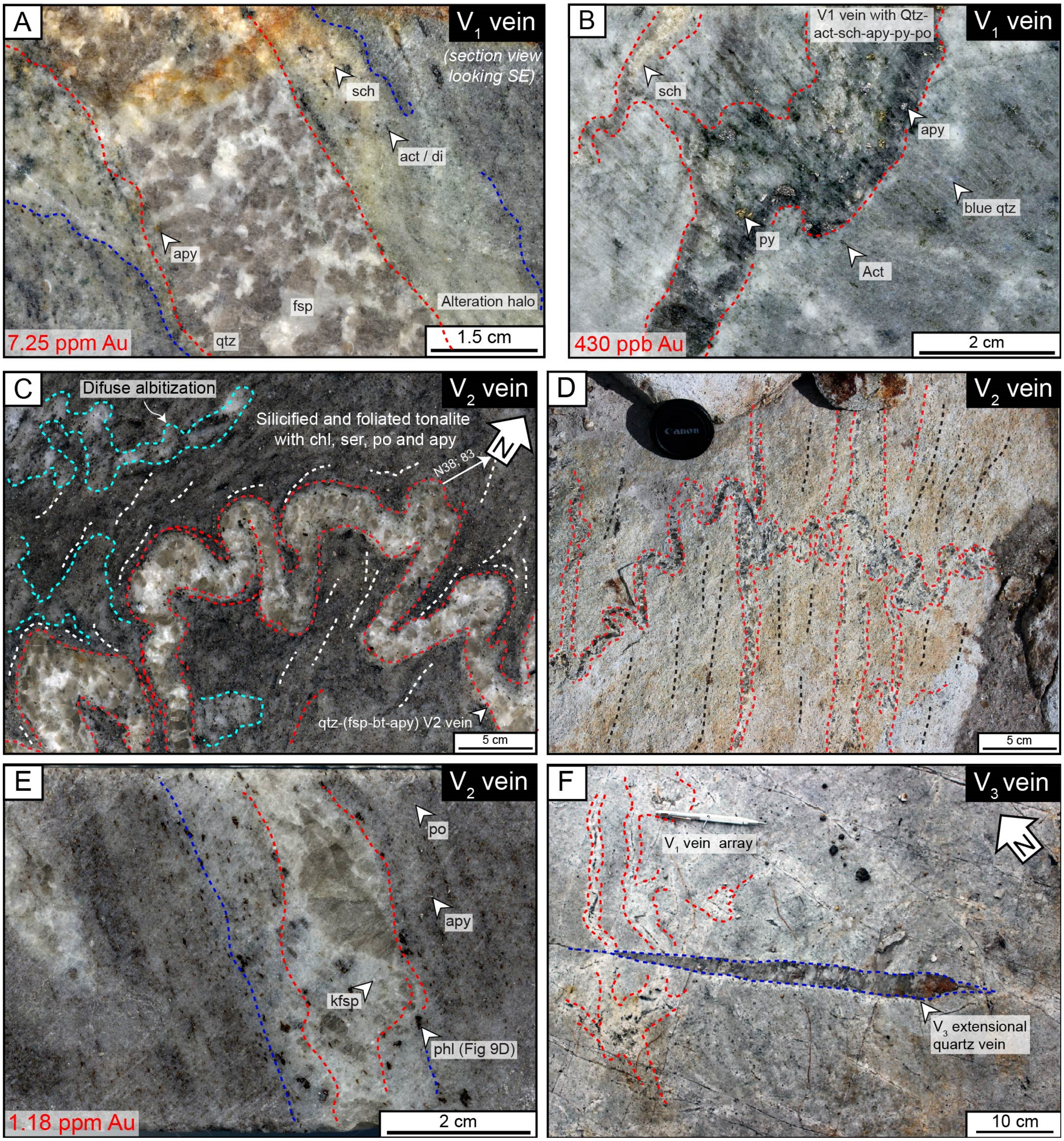

Figure 8: Macroscopic features of the auriferous vein network in the Cheechoo intrusion. A and B) V_1 veins composed of a quartz, feldspar, scheelite, pyrite, arsenopyrite in altered intrusion (A: See Fig. 3 for location; B: CH-919-15-20, 60.2 meters). C) Pegmatitic V_2 vein affected by ptygmatitic fold in gneissic intrusion (See Fig. 3 for location). D) Folded sheeted extensional V_2 vein array (main stripped area). E) V_2 vein composed of quartz, feldspar, coarse phlogopite, albite, arsenopyrite and pyrrhotite (CH-919-13-10, 49.6 meters). F: V_3 extensional vein cutting V_1 vein network (main stripped area). Ab: Albite, Apy: Arsenopyrite, Bt: Biotite, Qtz: Quartz, Phl: Phlogopite, Sch: Scheelite, Act: Actinolite; Di: Diopside, Py: Pyrite.

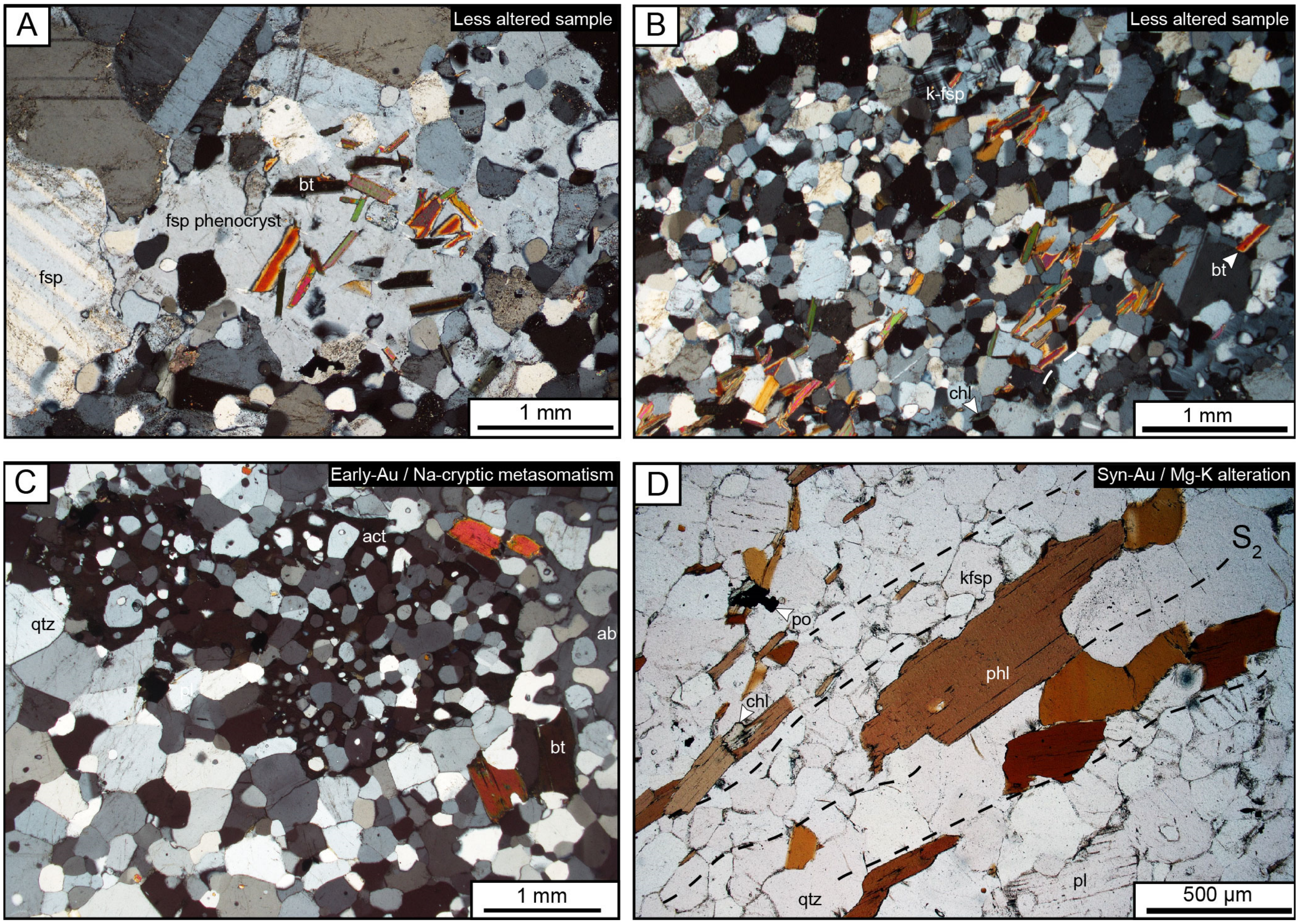

Figure 9: Petrographic features of fresh (A and B) and altered (C and D) Cheechoo intrusion samples. A) Feldspar phenocrysts in a matrix of feldspar, quartz and biotite (drill hole CH-919-13-10, 294 m; 0.26 ppm Au). B) Foliated intrusion with foliation-parrallel biotite porphyroblasts in a matrix of feldspar and quartz (drill hole CH-919-13-10, 294 m; 0.26 ppm Au). C) Na metasomatism characterized by the presence of secondary albite, actinolite and biotite (6-9 trench; see Fig. 4 for location). D) Phlogopite porphyroblasts with k-feldspar in a selvage of a V_2 vein in gneissic intrusion with local chlorite and pyrrhotite grains (drill hole CH-919-13-10; 49.6m; 1.18 ppm Au).

The first type of hydrothermal alteration is a "cryptic" Na-metasomatism marked by secondary interstitial albite and actinolite porphyroblasts (Fig. 9C) and illustrated by elevated Na_2O/Al_2O_3 molar ratio (Fig. 10A). The cryptic nature refers to the alteration terminology for the Fort Knox deposit, defined by Thompson and Newberry (2000). The CaO contents are similar to less altered samples (Table 1), suggesting that calcic feldspars have been replaced by actinolite without Ca input. This alteration assemblage is cut by the auriferous veins network and by pegmatite dykes suggesting an early-Au stage of alteration. Those samples show a Na_2O increase of 15 % and a 30% depletion in K_2O in association with drastic increases in Au (170 ppb Au), As, Te and Se (Fig. 10B). The second type of alteration is composed of variable proportions of opalescent quartz, phlogopite, sericite and microcline (Figs. 8E and 9D), commonly associated with disseminated sulphide (e.g. pyrrhotite, arsenopyrite). Phlogopite grains are coarser towards the V_2 vein network and characterized by high Ti (0.204 to 0.303 apfu), Mg# (0.57 to 0.73) and F contents (0.101 to 0.367 apfu). Those altered samples show increases in MgO (+30%) and K_2O (+20%), and decrease in Na_2O (-25%), in association with major increase in Au (285 ppb Au), As, Se, Te and Bi (Fig. 10C). The higher proportion of coarse phlogopite and, to a lesser extent, microcline near auriferous veins is illustrated by MgO and K_2O enrichments (Fig. 9D). The analyzed V_1 vein is characterized by a Bi-W-As ± (Te, Se, Pb) metallic signature (Fig. 10D), probably related to the presence of scheelite and composite grains of pyrrhotite, arsenopyrite and pyrite.

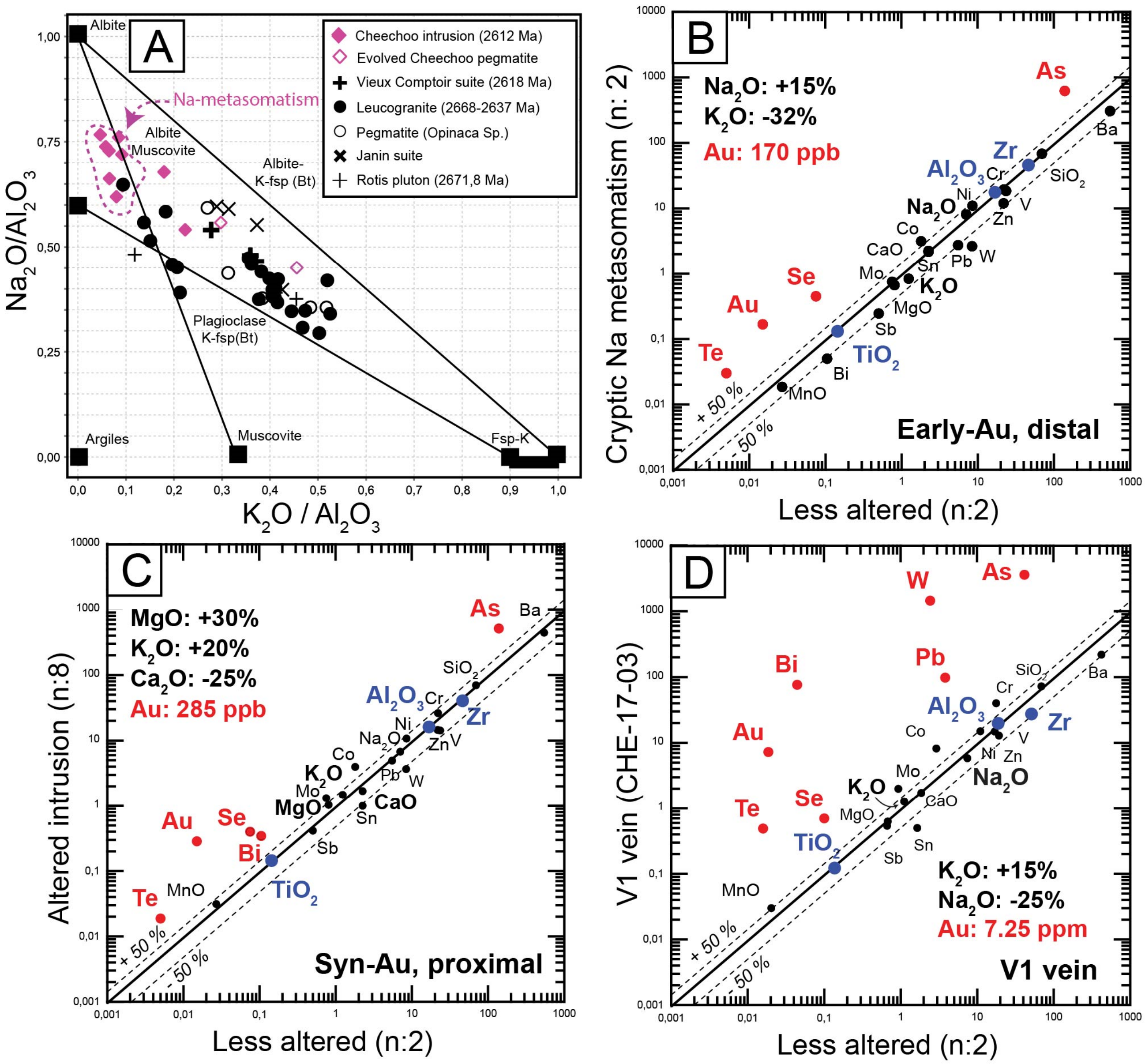

Figure 10: A) Na_2O/Al_2O_3 versus K_2O/Al_2O_3 molar ratio diagram, after Davies and Whitehead (2010). B, C and D) Isocon diagrams for distal and proximal hydrothermal alterations and a V_1 vein from Fig. 8A, based on the method defined by Grant (1986). See Fig. 9 for petrographic observations and Table 1 for geochemical data.

Sulphide mineralogy and sulfur isotope composition

Gold-associated sulphide grains are mainly arsenopyrite, pyrite, and pyrrhotite present within quartz veins or their alteration halos. Those sulphides vary in size from 100 µm (vein selvages) to 1 mm (veins) and locally occur as composite grains (e.g. arsenopyrite with pyrrhotite inclusions), with annealed or reactional textures (Fig. 11). Those sulphides are often associated with sericite and phlogopite (Fig. 9D and Fig. 11). Two samples were analyzed for sulfur isotope composition of gold-associated sulphides (Fig. 11). The first sample is a V_1 vein with quartz, feldspar, scheelite in the altered Cheechoo intrusion (Fig. 11A) and the second is a biotite-rich gneissic intrusion containing a V_2 vein composed of quartz ± (feldspar, phlogopite, arsenopyrite, pyrrhotite) (Fig. 11B). Values of in-situ $\delta^{34}S$ analyses ($^{34}S/^{32}S$ per mil) of gold-associated sulphides such as pyrite (n: 1), pyrrhotite (n: 4) and arsenopyrite (n: 9) are between –2.8 and 4.3, with a mean value of 1.19 (SEM= 1.86). Arsenopyrite values of the V_1 vein are slightly higher than those of the V_2 vein.

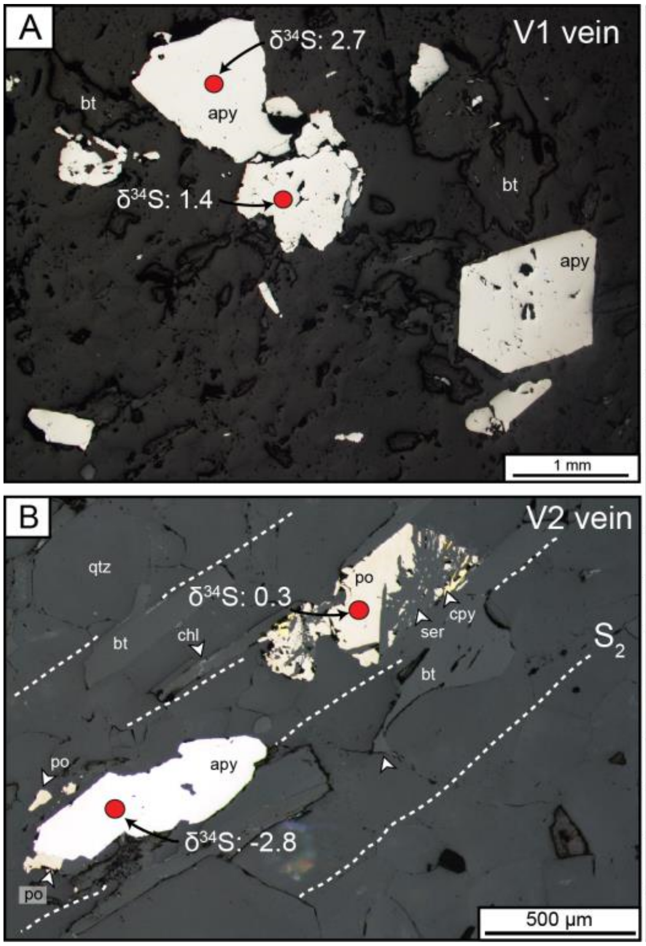

Mineral	Localisation	$\delta^{34}S_{VCDT}$	SD
Apy	V1 vein	4,3	
Apy	V1 vein	3,3	
Apy	V1 vein	2,7	
Apy	V1 vein	1,4	
Apy	V1 vein	2,6	
Apy	V2 vein	2,2	
Apy	V2 vein	-2,8	
Apy	V2 vein	-0,3	
Apy	V2 vein	2,3	
Mean Apy		**1,7**	1,5
Po	V2 vein	-0,1	
Po	V2 vein	0,4	
Po	V2 vein	0,3	
Po	V1 vein	1	
Mean Po		**0,4**	0,3
Pyrite	V1 vein	-0,6	
Mean sulfides		1,33	1,5

Figure 11: Sulfur isotope data from two mineralized samples. A) V_1 vein in altered intrusion. B) V_2 vein in recrystallized and gneissic biotite-rich intrusion. Abbreviations: Apy: Arsenopyrite, Bt: Biotite, Chl: Chlorite, Cpy: Chalcopyrite, Qtz: Quartz, Po: Pyrrhotite, Ser: Sericite. $\delta^{34}S$ values are standardized with Vienna Canyon Diablo Troilite standard.

DISCUSSION

The auriferous quartz, feldspar vein network (V_1 to V_3 veins) is better developed in deformed areas of the Cheechoo intrusion near its margins (in dilatational domains), and is spatially associated with pegmatite dykes. The current data suggests that gold grades of the vein network increase near pegmatite dykes and towards the intrusion margins. On the 6-9 trench, gold mineralization is associated with the vein network controlled by discrete E- to NE-trending high-strain zones (Fig. 4). To the north of the trench (Fig. 4), the vein network is progressively asymmetrically folded and transposed to the northeast due to late-D_2 to D_3 shear deformation. On the northern part of the main stripped area (Fig. 3), near the eastern edge of the intrusion, D_3 deformation transposes the S_2 foliation and the vein network into a NNW-striking orientation. The gold-bearing vein network is thus interpreted to have developed during D_2, and before D_3 deformation (Fig. 12).

The Cheechoo intrusion has a granodioritic to trondjemitic composition. The geochemistry of the Cheechoo intrusion indicates similarities with some leucogranites from the Opinaca Subprovince formed by partial melting of metagreywacke and/or TTG source(s). The geochemical signature of the Cheechoo intrusion is probably related to i) primary processes such as depth of melting, source of melts and ii) secondary processes such as fractional crystallization and hydrothermalism (Figs. 6 and 10). According to Fontaine et al. (2017b), the Cheechoo intrusion has a reduced nature ($Fe_2O_3/FeO < 0.2$) with high FeO+MnO contents.

Comparisons with the Éléonore gold mineralization and reduced intrusion-related gold systems

The Cheechoo gold mineralization shares some similarities with Éléonore gold mineralization including: i) the proximity to the Opinaca-La Grande tectono-metamorphic boundary, ii) a mineralization style dominated by a stockwork of quartz veins and veinlets, and the local presence auriferous pegmatitic quartz-feldspar veins and pegmatites in paragneiss, iii) the pre-D_3 development of the auriferous gold system (Fig. 12), and iv) a Mg-K hydrothermal footprint. The overprinting effects of deformation and metamorphism on the texture of the ore and alteration assemblages are common to both deposits, suggesting that the timing of mineralization is pre-peak metamorphism. Gold mineralization may be part of a large-scale auriferous system spanning ca. 5-10 Ma during the the D_2 deformation (Fig. 12). In-situ $\delta^{34}S$ sulphide data are similar to those from late Archean orogenic gold deposits (McCuaig and Kerrich, 1998), and to bulk $\delta^{34}S$ rock from granitoid-related gold mineralization (Yang and Lentz, 2010). Those values are also analogous to results obtained from sulphides at the Éléonore gold mine (Fontaine et al., 2017a). The presence of pyrrhotite and arsenopyrite as main gold-associated sulphides is compatible with a source of gold originating from a dominantly reduced ore fluid of metamorphic and/or magmatic origin(s) (McCuaig and Kerrich, 1998)

The hydrothermal and gold mineralization features of the Cheechoo property, temporal and/or spatial association with a reduced intrusion, pegmatites and mafic enclaves or dykes (Fig. 12) shares analogies with reduced intrusion-related gold systems (Thompson and Newberry, 2000; Hart, 2007). The composition of the Cheechoo intrusion share similarities with reduced ilmenite series and gold-associated granitoids (Fontaine et al., 2017b) described in Yukon, and Alaska (Hart et al., 2004) and in New Brunswick (Yang et al., 2008). In New Brunswick Appalachians, Yang et al. (2008) have proposed that intrusion-related gold systems are controlled by magmas sources, magmatic processes, redox conditions (country-rock nature), and local structural regimes. As suggested by Hart et al. (2004), the nature of the host rocks and the redox state of the magma is the most important factor controlling the metallogeny of intrusion-related ore systems. Particularly, during fractionation, redox features controlled the behaviour of metals (Ishihara, 1981; Hart et al., 2004). The crosscutting relationship between vein types can be explained by temperature variations and a possible steep thermal gradients on fluid chemistry, as described in details by Hart (2007). In this scenario, V_1 veins, could have formed at 400-300°C, just below the brittle-ductile transition, whereas V_2, V_2', V_3 veins were later emplaced at 250-300°C (Hart, 2007). According to Thompson and Newberry (2000), the early feldspathic alteration stage followed by a younger sericite-carbonate alteration, a feature described at Cheechoo (Fig. 10), could illustrate the shift in sulphidation state from pyrite-pyrrhotite (early, Au poor) to pyrite-arsenopyrite (late, Au-rich).

CONCLUDING REMARKS

The Cheechoo property (Sirios Resources) is located in the Eeyou Istchee Baie-James municipality, 15 km southeast of the Éléonore gold mine. The study area straddles the boundary between the Opinaca Subprovince to the north and the La Grande Subprovince to the south. The area is characterized by paragneiss and migmatites, syn- to late-tectonic intrusions, leucogranitic pegmatites, conglomerates, iron-rich formations and amphibolites. The 2612 Ma Cheechoo intrusion is emplaced in metasedimentary rocks of the Low Formation during the D_2 deformation and amphibolite facies metamorphism. The intrusion has a granodioritic, trondhjemitic, metaluminous and reduced composition with high Na_2O, FeO, LILE and low CaO and K_2O and HFSE contents. The Cheechoo intrusion has low magnetic susceptibilities with locally high magnetics domains at its margins. The intrusion is characterized by sacharoidal recrystallized to porphyritic textures with feldspar phenocrysts and biotite porphyroblasts in a matrix of quartz, feldspars, and biotite. The highly foliated domains near intrusion margins are associated with numerous leucogranitic pegmatites. The intrusion is affected by late- to post-emplacement high-strain zones and folds related to the late-D_2 to D_3 deformation. The presence of chlorite and randomly oriented amphiboles in the paragneissic wacke suggests retrograde metamorphism.

The mapping and structural analysis of two trenches indicates that the auriferous vein network developed before the D_3 deformation, probably late during D_2, near margins of the Cheechoo intrusion and in spatial association with pegmatite dykes. The auriferous sheeted vein network is composed of several types of veins: V_1 quartz ± (feldspar, scheelite, diopside, actinolite, pyrite-pyrrhotite, arsenopyrite), V_2 extensional to en-echelon quartz ± (feldspar, phlogopite, arsenopyrite, pyrrhotite), V_2' actinolite ± (feldspar, quartz) and V_3 quartz ± (actinolite) extensional veins. Quartz-feldspar veins with local coarse «pegmatitic» texture locally carry high-grade gold values at Cheechoo and also at the Moni prospect. The auriferous vein network is spatially associated with early-Au, distal Na-metasomatism (170 ppb Au) and syn-Au, proximal K-Mg metasomatism (285 ppb Au), as well as a Bi-W-As ± (Te, Se, Sb) metallic signature. These features share analogies with reduced intrusion-related gold systems.

Gold mineralization occurred during long-lived tectonometamorphic event(s) intimately associated with the emplacement of the Cheechoo reduced intrusion and a swarm of leucogranitic pegmatites within metasedimentary rocks near a Subprovince boundary, which are common features of Archean gold mineralization in metamorphosed and deformed terranes. Gold mineralization hosted by the 2612 Ma Cheechoo reduced intrusion is a new style of gold mineralization in the Éléonore gold mine area and elsewhere in the Eeyou Istchee Baie-James. The age and composition of the intrusion may represent a new regional metallotect, especially where occurring near the contact between the Opinaca and La Grande Subprovinces.

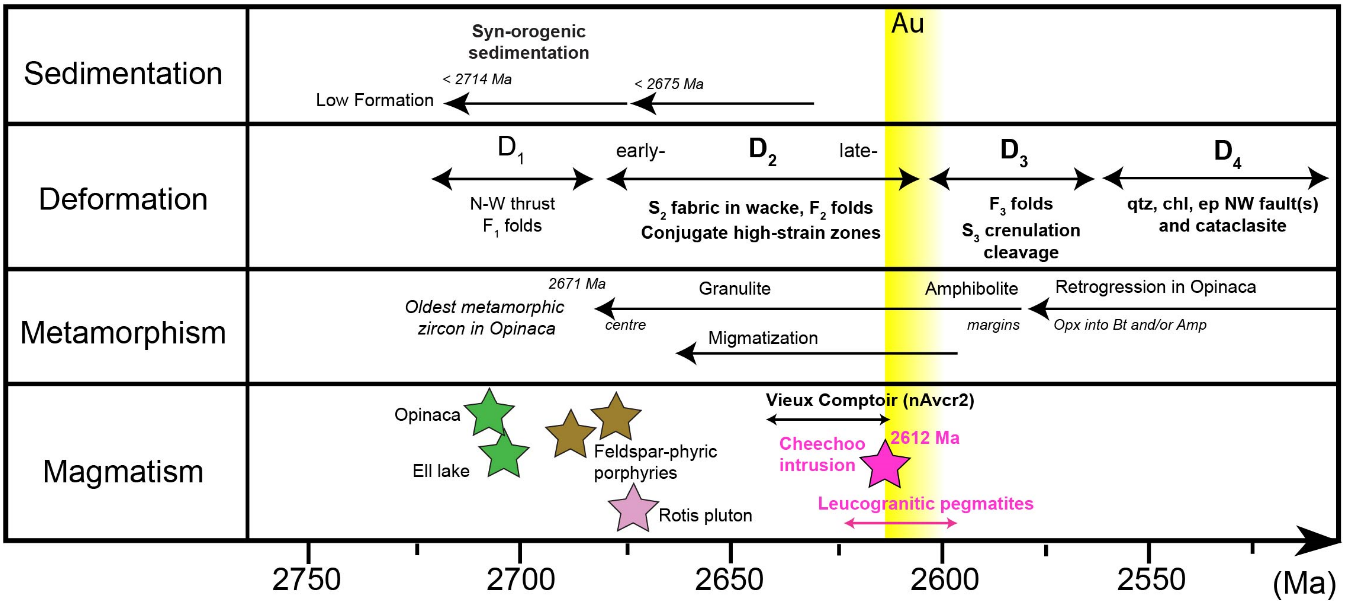

Figure 12: Schematic synthesis of sedimentation, deformation, metamorphism, magmatism and gold mineralization at Cheechoo. References: (Dubé et al., 2011); (Ravenelle et al., 2010); (Fontaine et al., 2015); (Goutier et al., 2000); (David et al., 2010); (Morfin et al., 2013); McNicoll V., unpublished; (Bandyayera and Fliszár, 2007); David, J., 2005, unpublished; (Goutier, 2017). The maximum age of the Cheechoo gold mineralization is constrained by the 2612 Ma Cheechoo host intrusion. Abbreviations: Amp: Amphibole, Bt: Biotite, Chl: Chlorite, Ep: Epidote, Opx: Orthopyroxene, Qtz: Quartz.

.ACKNOWLEDGMENTS

This research would not have been possible without the full support of Sirios Resources and its staff for scientific input and logistical support during fieldwork. We particularly thank Vincent Raymond, Nathalie Schnitzler Guillaume Doucet and Philippe Allard. Michel Gauthier and Jocelyn Pelletier are acknowledged for discussions that improved our understanding of the Cheechoo property. The collaboration of Glenn Piercey and Graham Layne (Memorial University) for sulfur isotope analyses is gratefully acknowledged. We thank Jean Goutier for sharing his knowledge of the Eeyou Istchee Baie-James geology and Morgane Gigoux and Stéphane de Souza for discussions on the Cheechoo geology. The study was funded through Geological Survey of Canada's Targeted Geoscience Initiative. Goldcorp-Éléonore, The Fond de Recherche du Québec – Nature et Technologies (FRQNT) and the Natural Sciences and Engineering Research Council of Canada (NSERC) are also thanked for providing a scholarship to the first author through the Industrial Innovation Scholarships program. A. Fontaine would like to thank AQUEST and DIVEX for their financial support through scholarships. This report benefited from the review of Sébastien Castonguay.

REFERENCES

Azimut (2017) Azimut intersects 4.9 g/t Au over 45.0m at Eleonore South, James Bay region, Quebec http://www.azimut-exploration.com/en/release/PR_20170502.pdf.

Bandyayera D, Fliszár A (2007) Géologie de la région de la baie Kasipasikatch (33C09) et du lac Janin (33C16), MRNF, RP 2007-05.

Bandyayera D, Lacoste P (2009) Géologie de la région du lac de Rotis (33C10), du lac Bernou (33C11) et du lac Boyd (33C15), Ministère de l'Énergie et des Ressources naturelles, RP-2009-06.

Bandyayera D, Rhéaume P, Maurice C, Bédard É, Morfin S, Sawyer E (2010) Synthèse géologique du secteur du réservoir Opinaca, Baie-James, MRNF, RG 2010-02.

Barnicoat AC, Fare RJ, Groves DI, McNaughton NJ (1991) Synmetamorphic lode-gold deposits in high-grade Archean settings. Geology 19(9):921-924.

Card K (1990) A review of the Superior Province of the Canadian Shield, a product of Archean accretion. Precambrian Research 48(1-2):99-156.

Card K, Ciesielski A (1986) Subdivisions of the Superior Province of the Canadian shield. Geoscience Canada 13(1).

Colvine A (1989) An empirical model for the formation of Archean gold deposits: products of final cratonization of the Superior Province, Canada. Economic Geology Monograph 6:37-53.

Condie KC (1981) *Archean greenstone belts.* Elsevier,

Couture J, Guha J (1990) Relative timing of emplacement of an Archean lode-gold deposit in an amphibolite terrane: the Eastmain River deposit, northern Quebec. Canadian Journal of Earth Sciences 27(12):1621-1636.

David J, Parent M (1997) Géochronologie U-Pb du Projet Moyen-nord, GM59903, 88 pages. :88.

David J, Vaillancourt D, Bandyayera D, Simard M, Dion C, Goutier J, Barbe P (2010) Datations U-Pb effectuées dans les sous-provinces d'Ashuanipi, de La Grande, d'Opinaca et d'Abitibi en 2008–2009, MRNF, Québec, RP 11, 37p.

Davies J, Whitehead R (2010) Alkali/alumina molar ratio trends in altered granitoid rocks hosting porphyry and related deposits. Exploration and Mining Geology 19(1-2):13-22.

Dubé B, Gosselin P (2007) Greenstone-hosted quartz-carbonate vein deposits. Mineral Deposits of Canada: A synthesis of major deposit-types, district metallogeny, the evolution of geological provinces, and exploration methods: Geological Association of Canada, Mineral Deposits Division, Special Publication 5:49-73.

Dubé B, Mercier-Langevin P, Castonguay S, McNicoll V, Bleeker W, Lawley C, De Souza S, Jackson S, Dupuis C, Gao J, Bécu V, Pilote P, Goutier J, Beakhouse G, Yergeau D, Oswald W, Janvier V, Fontaine A, Pelletier M, Beauchamp A-M, Malo M, Katz L, Kontak D, Tóth Z, Lafrance B, Gourcerol B, Thurston P, Creaser R, Enkin R, El Goumi N, Grunsky E, Schneider D, Kelly C, Lauzière K (2015) Precambrian lode gold deposits - a summary of TGI-4 contributions to the understanding of lode gold deposits, with an emphasis on implications for exploration, Targeted Geoscience Initiative 4, Geological Survey Open File 7852. doi:10.4095/296624.

Dubé B, Ravenelle J-F, McNicoll V, Malo M, Creaser R, Nadeau L, Simoneau J (2011) The world-class Roberto gold deposit, Éléonore property, James Bay area, Québec: insights from geology and geochronology, Joint Annual Meeting of the GAC - MAC – SEG - SGA, Ottawa, Canada.

Fontaine A, Dubé B, Malo M, McNicoll V, Brisson T, Doucet D, Goutier J (2015) Geology of the metamorphosed Roberto gold deposit (Éléonore mine), Baie-James region, Québec: diversity of mineralization styles in a polyphase tectono-metamorphic setting, in Targeting Geoscience Initiative 4, Geological Survey of Canada Open File 7852.

Fontaine A, Dubé B, Malo M, McNicoll V, Jackson SE, Beausoleil C, Layne GD, Goutier J (2017a) Geology and insights on the genesis of the world-class Éléonore gold mine, Eeyou Istchee Baie-James, Superior Province, Quebec, Canada In: Proceeding of the 14th Biennial SGA Meeting, 20-23 August 2017, Québec, Canada, p. 31-34.

Fontaine A, Dubé B, Malo M, Ravenelle J-F, Fournier E, McNicoll VJ, Beausoleil C, Prud'homme N, Goutier J (2017b) The Éléonore gold mine: Exploration, Discovery and Understanding of an emerging gold district in Eeyou Istchee James Bay, Superior Province, Northern Québec, Canada; in Proceedings of Exploration 17: Sixth Decennial International Conference on Mineral Exploration, (ed.) V. Tschirhart and M.D. Thomas; Decennial Minerals Exploration Conferences, Toronto, Ontario, p.601-617.

Franconi A (1978) La bande volcanosédimentaire de la rivière Eastmain inférieure. Édit Québec MDRND), p 59.

Galley AG, Lafrance B (2014) Setting and evolution of the Archean synvolcanic Mooshla intrusive complex, Doyon-Bousquet-LaRonde mining camp, Abitibi greenstone belt: Emplacement history, petrogenesis, and implications for Au metallogenesis. Economic Geology 109(1):205-229.

Gauthier M (2000) Styles et répartition des gîtes métallifères du territoire de la Baie-James (Québec). Chronique de la Recherche minière (No. 539).

Gauthier M, Larocque M (1998) Cadre géologique, style et répartition des minéralisation métalliques de la Basse et de la Moyenne Eastmain, Territoire de la Baie James. Édit Québec G (Governement of Quebec).

Gauthier M, Trépanier S, Gardoll S (2007) Metamorphic gradient: A regional-scale area selection criterion for gold in the northeastern Superior province, eastern Canadian Shield. Society of Economic Geologists Newsletter 69:10-15.

Goldfarb RJ, Baker T, Dube B, Groves DI, Hart CJ, Gosselin P (2005) Distribution, character, and genesis of gold deposits in metamorphic terranes. Economic Geology 100th anniversary volume 40.

Goutier J (2017) Géologie de la région du lac Ewart, sous-provinces de La Grande et d'Opinaca, à l'est de Radisson, Municipalité Eeyou Istchee Baie-James, Québec, Canada, http://gq.mines.gouv.qc.ca/bulletins-geologiques/lac-ewart/.

Goutier J, Dion C, Lafrance I, David J, Parent M, Dion D (1999) Géologie de la région des lacs Langelier et Threefold (SNRC 33F/03 et 33F/04). Ministère des Ressources naturelles, Québec, RG :98-18.

Goutier J, Dion C, Ouellet M, David J, Parent M (2000) Géologie de la région des lacs Guillaumat et Sakami (SNRC 33F/02 et 33F/07): MRNF, Québec, Report RG 99-15, 37 p.

Goutier J, Dion C, Ouellet M, Mercier-Langevin P, Davis D (2001) Géologie de la région de la colline Masson (33F/09), de la passe Awapakamich (33F/10), de la baie Carbillet (33F/15) et de la passe Pikwahipanan (33F/16). Ministère des Ressources naturelles, Québec :2000-2010.

Grant JA (1986) The isocon diagram; a simple solution to Gresens' equation for metasomatic alteration. Economic Geology 81(8):1976-1982.

Groves D (1993) The crustal continuum model for late-Archaean lode-gold deposits of the Yilgarn Block, Western Australia. Mineralium deposita 28(6):366-374.

Groves D, Knox-Robinson C, Ho S, Rock N (1990) An overview of Archaean lode-gold deposits. Gold deposits of the Archaean Yilgarn Block, Western Australia: nature, genesis and exploration guides 20:2-18.

Hart CJ (2007) Reduced intrusion-related gold systems. Mineral Deposits of Canada: A synthesis of Major deposit types, district metallogeny, the Evolution of geological provinces, and exploration methods: Geological Association of Canada, Mineral Deposits Division, Special Publication 5:95-112.

Hart CJ, Mair JL, Goldfarb RJ, Groves DI (2004) Source and redox controls on metallogenic variations in intrusion-related ore systems, Tombstone-Tungsten Belt, Yukon Territory, Canada. Transactions of the Royal Society of Edinburgh: Earth Sciences 95(1-2):339-356.

Hocq M (1994) La Province du Supérieur dans Géologie du Québec. 94(1).

Ishihara S (1981) The granitoid series and mineralization Economic Geolology 75th Anniversary Volume. :458-484.

Jahn B-M, Glikson A, Peucat J, Hickman A (1981) REE geochemistry and isotopic data of Archean silicic volcanics and granitoids from the Pilbara Block, Western Australia: implications for the early crustal evolution. Geochimica et Cosmochimica Acta 45(9):1633-1652.

Kamb WB (1959) Ice petrofabric observations from Blue Glacier, Washington, in Relation to Theory and Experiment. Journal of Geophysical Research 64(11).

Laurent O, Martin H, Moyen J-F, Doucelance R (2014) The diversity and evolution of late-Archean granitoids: Evidence for the onset of "modern-style" plate tectonics between 3.0 and 2.5 Ga. Lithos 205:208-235.

Low AP (1896) Report on explorations in the Labrador Peninsula along the East Main, Koksoak, Hamilton, Manicuagan and portions of others rivers in 1892-93-94-95, Geological Survey of Canada, Annual Report vol. 8, (1895), pt. L, 1896; 387 pages (4 sheets), doi:10.4095/293888.

Maniar PD, Piccoli PM (1989) Tectonic discrimination of granitoids. Geological society of America bulletin 101(5):635-643.

McCuaig TC, Kerrich R (1998) P—T—t—deformation—fluid characteristics of lode gold deposits: evidence from alteration systematics. Ore Geology Reviews 12(6):381-453.

McDonough WF, Sun S-S (1995) The composition of the Earth. Chemical geology 120(3-4):223-253.

Morfin S, Sawyer E, Bandyayera D (2013) Large volumes of anatectic melt retained in granulite facies migmatites: An injection complex in northern Quebec. Lithos 168:200-218.

Morfin S, Sawyer EW, Bandyayera D (2014) The geochemical signature of a felsic injection complex in the continental crust: Opinaca Subprovince, Quebec. Lithos 196:339-355.

Moukhsil A (2000) Géologie de la région des lacs Pivert (33C/01), Anatacau (33C/02), Kauputauchechun (33C/07) et Wapamisk (33C/08), Ministère des Ressources naturelles, Québec; RG 2000-04, 47 pages, 4 plans.).
Moukhsil A, Legault M, Boily M, Doyon J, Sawyer E, Davis DW (2003) Synthèse géologique et métallogénique de la ceinture de roches vertes de la Moyenne et de la Basse-Eastmain (Baie-James), Ministère des Ressources naturelles, de la Faune et des Parcs, Québec; ET 2002-06, 55 pages, 1 plan.
Neumayr P, Cabri L, Groves D, Mikucki E, Jackman J (1993) The mineralogical distribution of gold and relative timing of gold mineralization in two Archean settings of high metamorphic grade in Australia. The Canadian Mineralogist 31(3):711-725.
O'connor J (1965) A classification for quartz-rich igneous rocks based on feldspar ratios. US Geological Survey Professional Paper B 525:79-84.
Percival J, Stern R, Skulski T, Card K, Mortensen J, Begin N (1994) Minto block, Superior province: Missing link in deciphering assembly of the craton at 2.7 Ga. Geology 22(9):839-842.
Percival JA, Skulski T, Sanborn-Barrie M, Stott GM, Leclair AD, Corkery MT, Boily M (2012) Geology and tectonic evolution of the Superior Province, Canada. Tectonic Styles in Canada: The LITHOPROBE Perspective. Edited by JA Percival, FA Cook, and RM Clowes. Geological Association of Canada Special Paper 49:321-378.
Percival JA, Stern RA, Rayner N (2003) Archean adakites from the Ashuanipi complex, eastern Superior Province, Canada: geochemistry, geochronology and tectonic significance. Contributions to Mineralogy and Petrology 145(3):265-280.
Poulsen KH, Robert Fo, Dubé B (2000) *Geological classification of Canadian gold deposits.* Geological Survey of Canada Bulletin 540,
Ravenelle J-F (2013) Amphibolite facies gold mineralization: an exemple from the Roberto deposit, Eleonore property, James Bay, Quebec, Université du Québec, Institut national de la recherche scientifique, 325 p.
Ravenelle J-F, Dubé B, Malo M, McNicoll V, Nadeau L, Simoneau J (2010) Insights on the geology of the world-class Roberto gold deposit, Éléonore property, James Bay area, Quebec; Geological Survey of Canada, Current Research 2010-1, 26p.
Remick J (1977) Wemindji area (Municipiality of James Bay), Preliminary report, Ministère des Richesses naturelles, DPV-446.), p 51 pages, 14 plans.
Robert F, Poulsen KH, Cassidy KF, Hodgson CJ (2005) Gold metallogeny of the Superior and Yilgarn cratons. Economic geology 100:1001-1033.
Rock NM (1987) The nature and origin of lamprophyres: an overview. Geological Society, London, Special Publications 30(1):191-226.
Simard M, Gosselin C (1999) Géologie de la région du lac Lichteneger (SNRC 33B), Ministère des Ressources naturelles, RG 98-15, 25 pages, 1 plan.).
Sirios (2014) Two Gold Zones on CHEECHOO: 7.24 g/t Au Over 7.9 m and 1.53g/t Au Over 19.5m https://www.sirios.com/fr/press/2014/18.
Sirios (2016) Sirios Intersects 12.08 g/t Au over 20.3 metres by Drilling at Cheechoo https://www.sirios.com/en/press/2016/7.
Sirios (2017) Sirios intersects 11.9 g/t Au over 13.5 metres in drilling on Cheechoo https://www.sirios.com/en/press/2017/5.
Sirios (2018a) 56.4 g/t Au over 8.2 m, including 867.1 g/t Au over 0.5 m on the Jordi Zone at Cheechoo https://www.sirios.com/en/press/2018/7.
Sirios (2018b) Sirios confirms auriferous mineralization for 1,400 m along the tonalite/metasediment contact at CHEECHOO, https://www.sirios.com/en/press/2018/2.
Sirios (2018c) Sirios intersects a new zone of 41 g/t Au over 8 metres at Cheechoo https://www.sirios.com/fr/press/2018/3.
Sirios Inc (2016) Découverte aurifère Cheechoo, Eeyou Istchee Baie James, Xplor 2016, 6 Octobre 2016.
Stern RA, Percival JA, Mortensen JK (1994) Geochemical evolution of the Minto block: a 2.7 Ga continental magmatic arc built on the Superior proto-craton. Precambrian Research 65(1-4):115-153.
Streckeisen A (1976) To each plutonic rock its proper name. Earth-science reviews 12(1):1-33.
Taylor WR, Rock NM, Groves DI, Perring CS, Golding SD (1994) Geochemistry of Archean shoshonitic lamprophyres from the Yilgarn Block, Western Australia: Au abundance and association with gold mineralization. Applied geochemistry 9(2):197-222.
Thompson J, Newberry R (2000) Gold deposits related to reduced granitic intrusions. Reviews in Economic Geology 13:377-400.
Thurston P (2002) Autochthonous development of Superior Province greenstone belts? Precambrian Research 115(1):11-36.
Turcotte J (2014) Campagne de forage d'exploration 2013 sur la propriété Cheechoo B Reservoir Opinaca, Baie James, Nord du Québec NTS33B/12 GM69038.
Vigneau S (2011) Métallogénie des minéralisations aurifères de la propriété Opinaca, Baie-James, Québec, Mémoire de maîtrise, Université de Québec à Chicoutimi, 307 pages.
Weinberg R, Searle M (1998) The Pangong Injection Complex, Indian Karakoram: a case of pervasive granite flowthrough hot viscous crust. Journal of the Geological Society 155(5):883-891.
Williams HR (1990) Subprovince accretion tectonics in the south-central Superior Province. Canadian Journal of Earth Sciences 27(4):570-581.
Winchester J, Floyd P (1977) Geochemical discrimination of different magma series and their differentiation products using immobile elements. Chemical geology 20:325-343.
Wyman D, Kerrich R (1993) Archean shoshonitic lamprophyres of the Abitibi Subprovince, Canada: petrogenesis, age, and tectonic setting. Journal of Petrology 34(6):1067-1109.
Yang X-M, Lentz DR (2010) Sulfur isotopic systematics of granitoids from southwestern New Brunswick, Canada: implications for magmatic-hydrothermal processes, redox conditions, and gold mineralization. Mineralium Deposita 45(8):795-816.
Yang X-M, Lentz DR, Chi G, Thorne KG (2008) Geochemical characteristics of gold-related granitoids in southwestern New Brunswick, Canada. Lithos 104(1):355-377.